

# Thrombosis and Haemostasis

## Iron-driven alterations on red blood cell-derived microvesicles amplify coagulation during hemolysis via the intrinsic tenase complex

Laura Delvasto, Dorina Roem, Kamran Bakhtiari, Gerard J van Mierlo, Joost Meijers, Ilse Jongerius, Sacha S Zeerleder.

Affiliations below.

DOI: 10.1055/a-1497-9573

Please cite this article as: Delvasto L, Roem D, Bakhtiari K et al. Iron-driven alterations on red blood cell-derived microvesicles amplify coagulation during hemolysis via the intrinsic tenase complex. *Thromb Haemost* 2021. doi: 10.1055/a-1497-9573

**Conflict of Interest:** The authors declare that they have no conflict of interest.

**This study was supported by** Trombosetiching Nederland (<http://dx.doi.org/10.13039/501100012028>), 201604, Stichting Sanquin Bloedvoorziening (<http://dx.doi.org/10.13039/501100012023>), PPOC19-24/L2467

### Abstract:

Hemolytic disorders characterized by complement-mediated intravascular hemolysis, such as autoimmune hemolytic anemia and paroxysmal nocturnal hemoglobinuria, are often complicated by life-threatening thromboembolic complications. Severe hemolytic episodes result in the release of red blood cell (RBC)-derived pro-inflammatory and oxidatively reactive mediators (e.g. extracellular hemoglobin, heme and iron) into plasma. Here, we studied the role of these hemolytic mediators in coagulation activation by measuring FXa and thrombin generation in the presence of RBC lysates. Our results show that hemolytic microvesicles (HMVs) formed during hemolysis stimulate thrombin generation through a mechanism involving FVIII and FIX, the so-called intrinsic tenase complex. Iron scavenging during hemolysis using deferoxamine decreased the ability of the HMVs to enhance thrombin generation. Furthermore, the addition of ferric chloride (FeCl<sub>3</sub>) to plasma propagated thrombin generation in a FVIII and FIX-dependent manner suggesting that iron positively affects blood coagulation. Phosphatidylserine (PS) blockade using lactadherin and iron chelation using deferoxamine reduced intrinsic tenase activity in a purified system containing HMVs as source of phospholipids confirming that both PS and iron ions contribute to the procoagulant effect of the HMVs. Finally, the effects of FeCl<sub>3</sub> and HMVs decreased in the presence of ascorbate and glutathione indicating that oxidative stress plays a role in hypercoagulability. Overall, our results provide evidence for the contribution of iron ions derived from hemolytic RBCs to thrombin generation. These findings add to our understanding of the pathogenesis of thrombosis in hemolytic diseases.

### Corresponding Author:

Laura Delvasto, Sanquin Research, Amsterdam, Netherlands, l.delvasto-nunez@sanquin.nl

### Affiliations:

Laura Delvasto, Sanquin Research, Sanquin Research, Amsterdam, Netherlands

Dorina Roem, Sanquin Research, Sanquin Research, Amsterdam, Netherlands

Kamran Bakhtiari, Sanquin Research, Plasma Proteins, Amsterdam, Netherlands

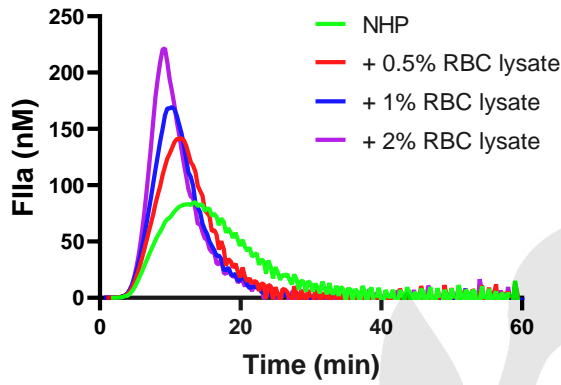
[...]

Sacha S Zeerleder, Academic Medical Center, Department of Hematology, Amsterdam, Netherlands

This is a PDF file of an unedited manuscript that has been accepted for publication. As a service to our customers we are providing this early version of the manuscript. The manuscript will undergo copyediting, typesetting, and review of the resulting proof before it is published in its final form. Please note that during the production process errors may be discovered which could affect the content, and all legal disclaimers that apply to the journal pertain.

# Figure 1

## A



## B

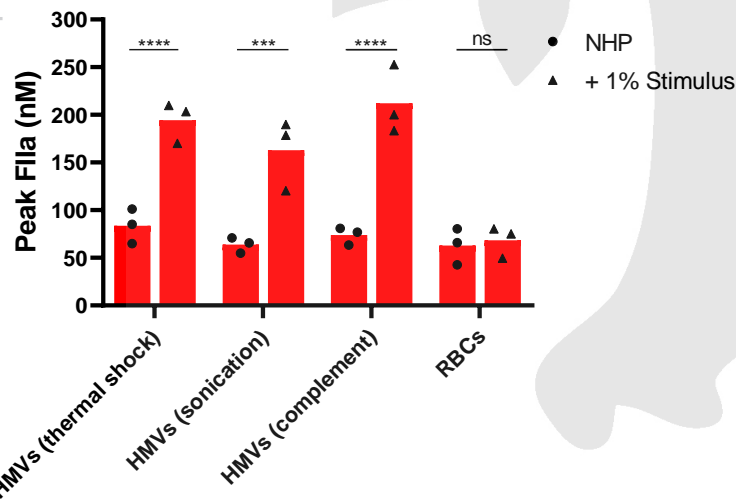
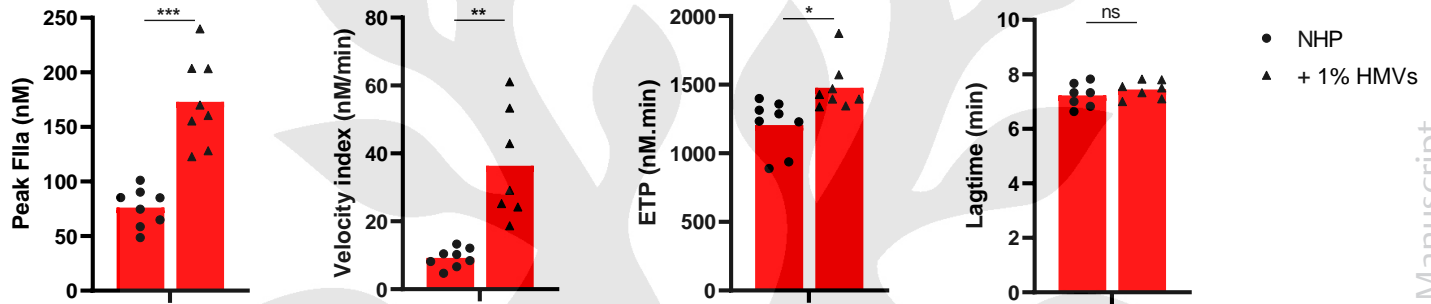
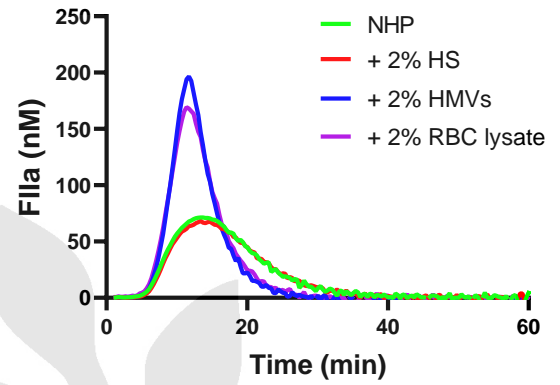


**Figure 2**

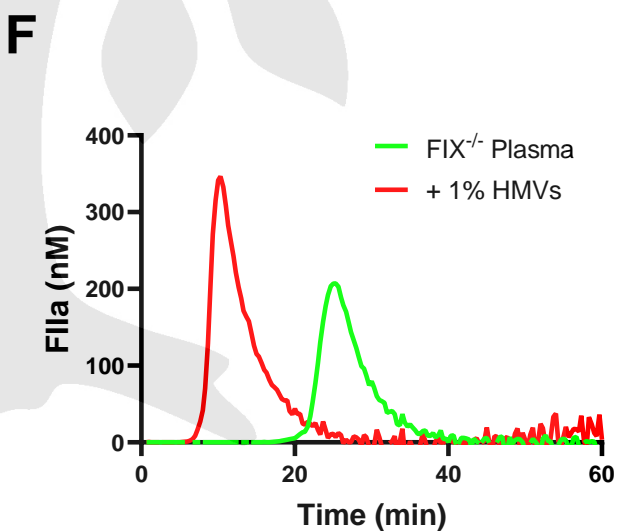
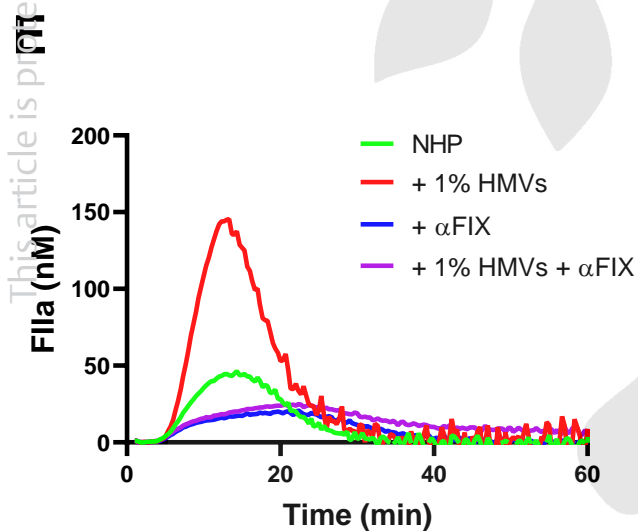
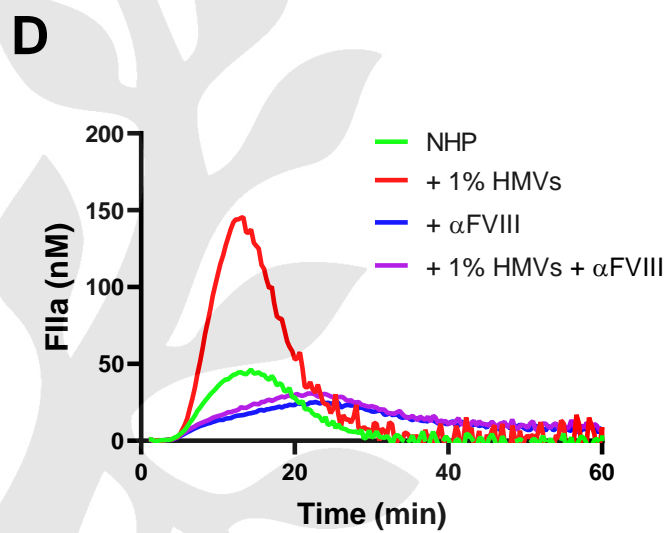
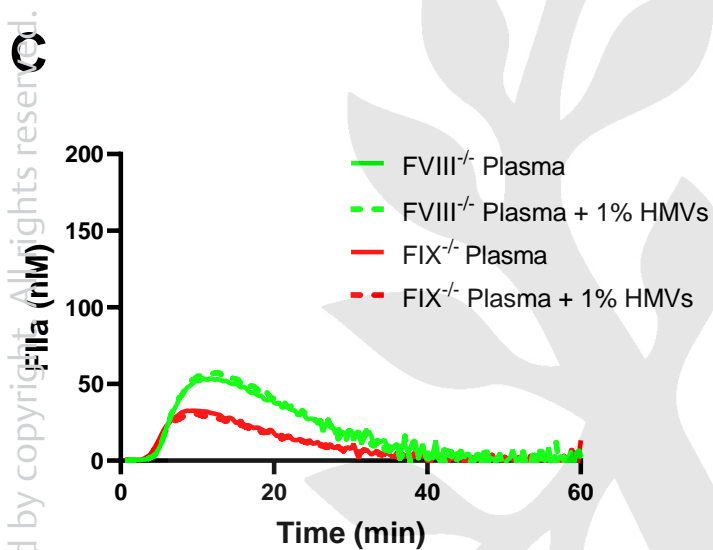
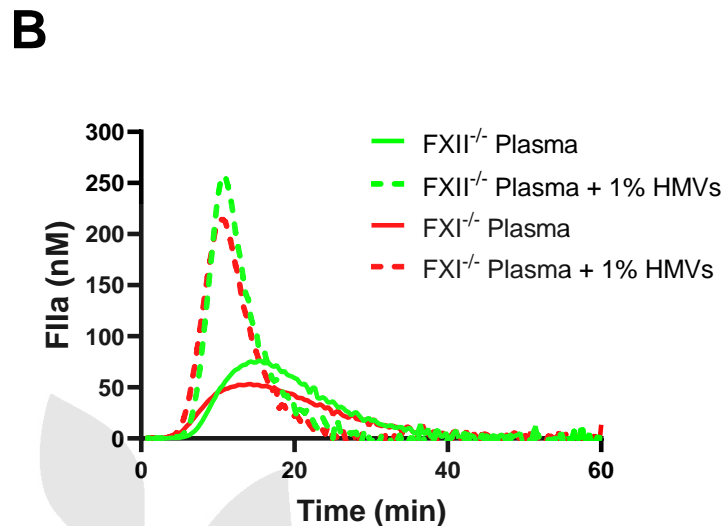
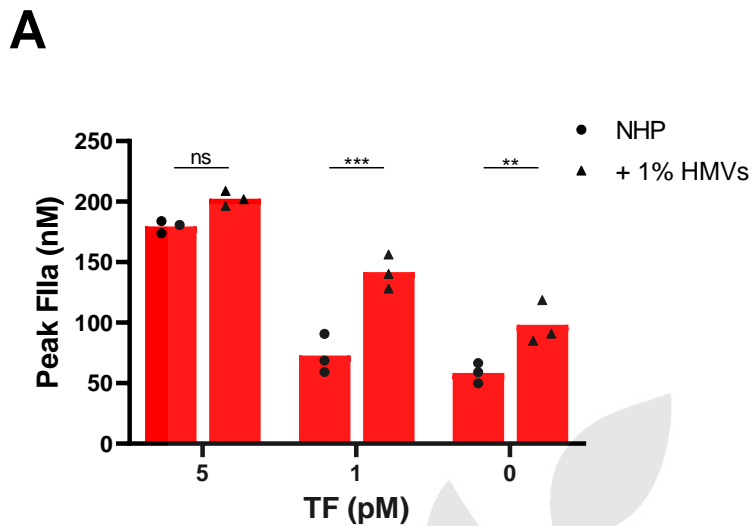
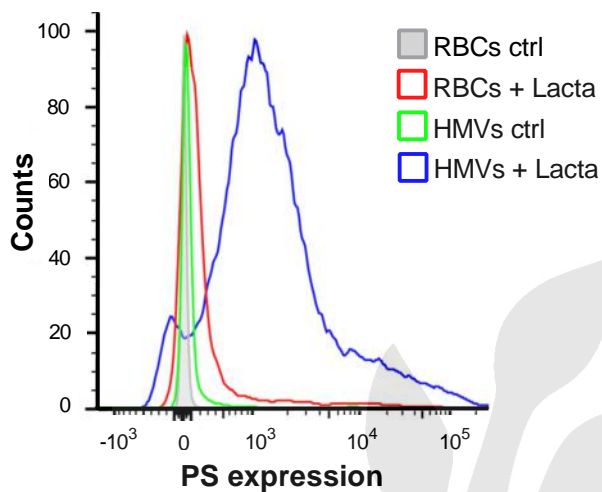
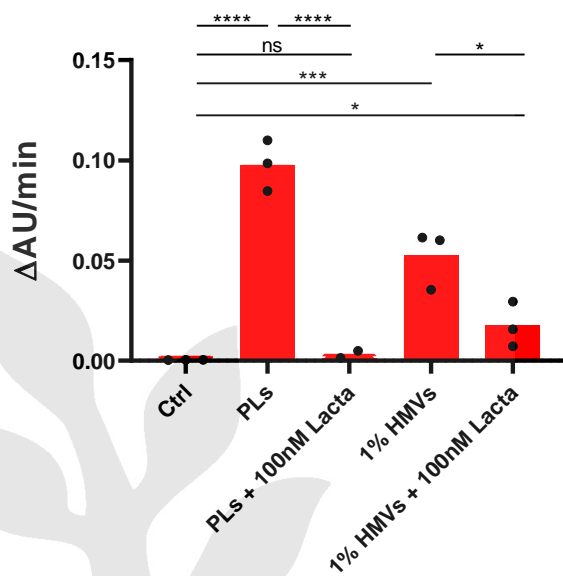


# Figure 3

## A



## B



## D

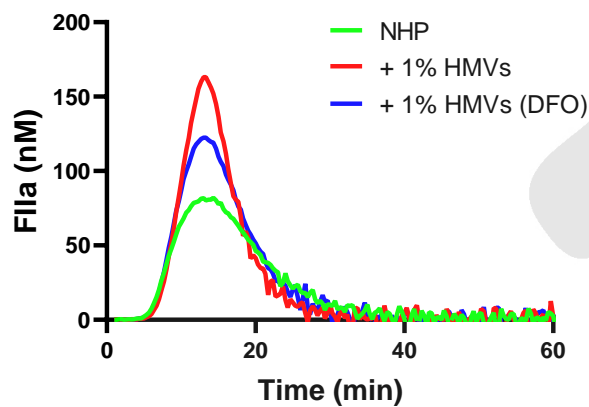
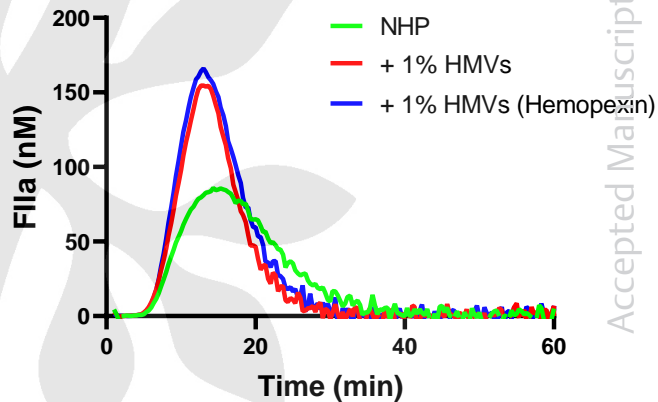
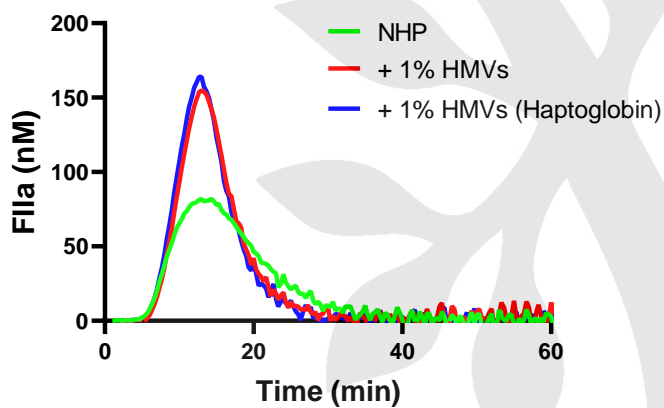
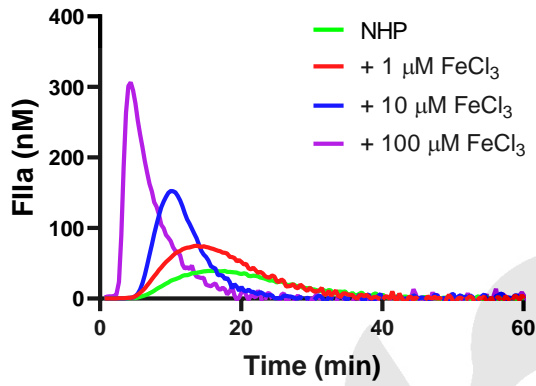
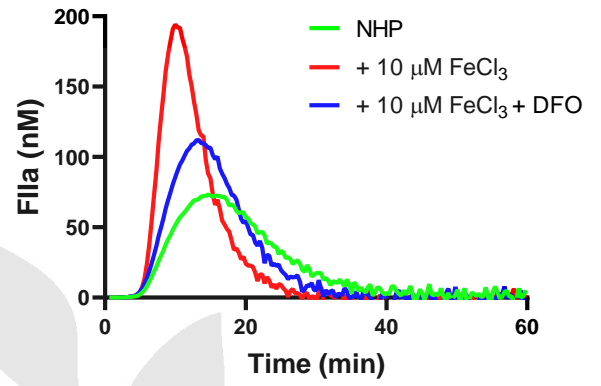


**Figure 4**

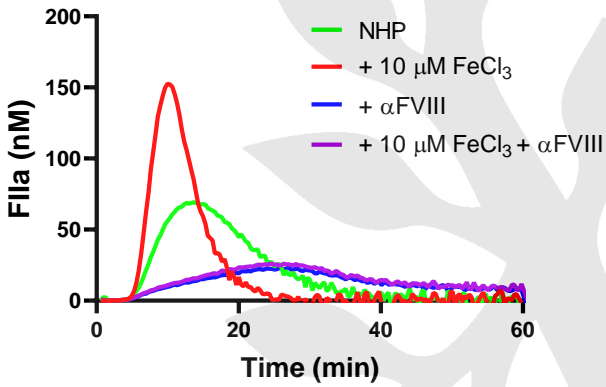
**A**



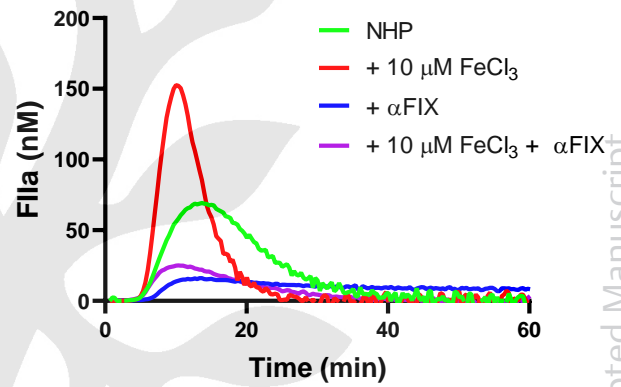
**B**



**C**



**D**



**E**

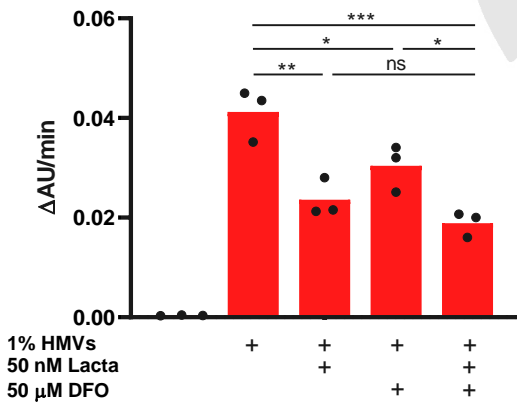
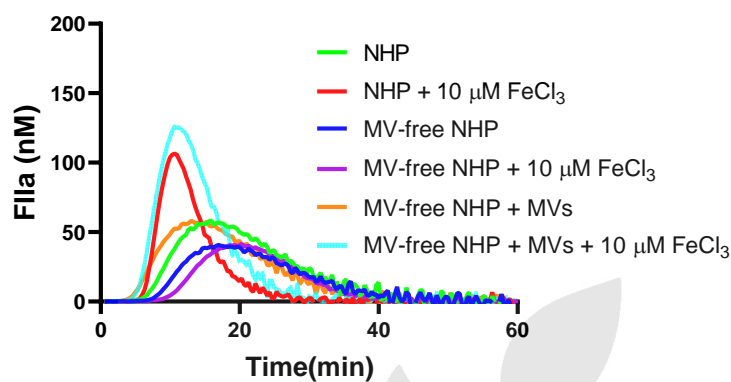
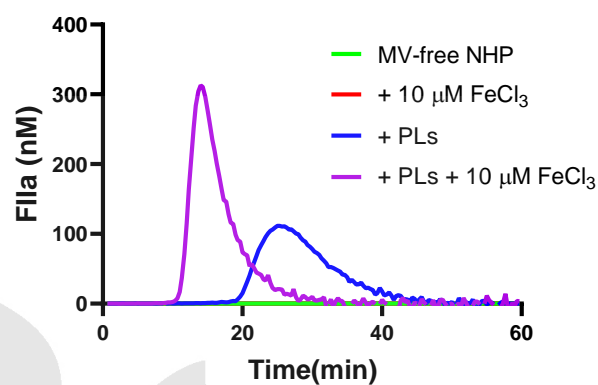


**Figure 5**

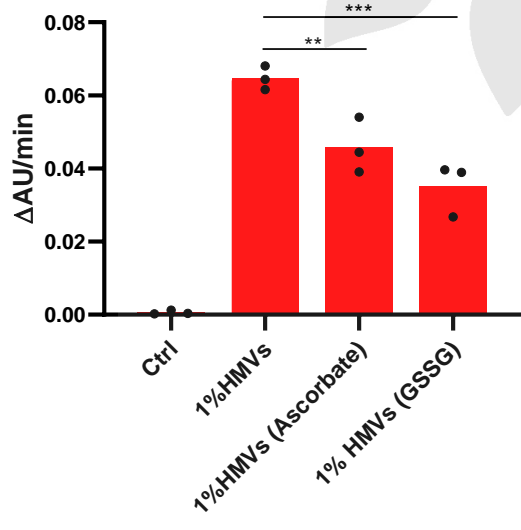
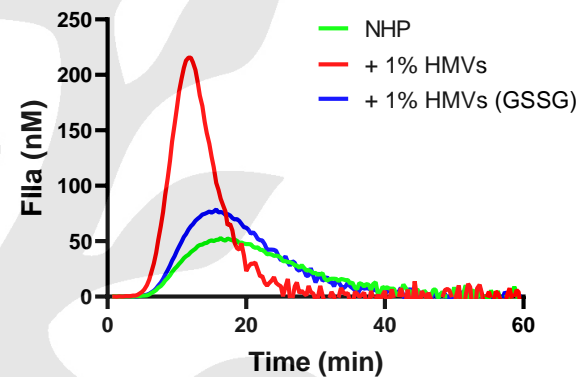
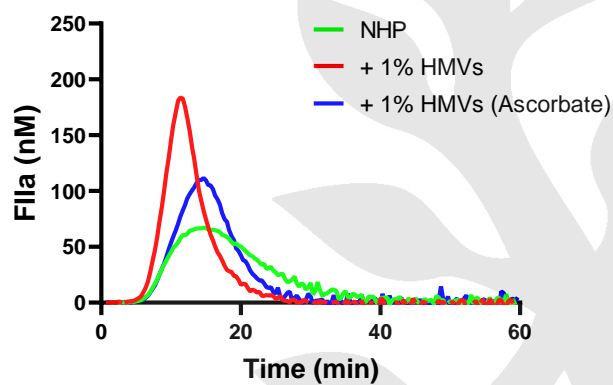
**A**



**B**



**D**



## Supplementary materials and methods

### *Purification of plasma-derived hemopexin*

Hemopexin was purified from human plasma using high-performance liquid chromatography (HPLC) on an AKTA avant 25 system (GE Healthcare). Fresh frozen plasma was thawed, pooled, and supplemented with 1 mM phenylmethylsulphonyl fluoride (PMSF). Then, the cryosupernatant was applied to a DEAE Sepharose Fast Flow column (5 × 30 cm) equilibrated with Buffer A (10 mM phosphate, pH 7.4). Flow rates of 10 mL/min were obtained. Bound hemopexin was washed with Buffer A to remove impurities, and subsequently eluted with 40 mM NaCl. Hemopexin in eluate fractions was determined by ELISA. The fraction containing hemopexin was supplemented with 500 mM NaCl and 10 mM imidazole, and applied with a flow rate of 5 mL/min to a Ni<sup>2+</sup>-charged immobilized metal affinity chromatography (IMAC) column (1.6 × 10 cm) equilibrated with Buffer B (10 mM phosphate, pH 7.4, containing 500 mM NaCl and 10 mM imidazole). The column was washed with Buffer B and bound hemopexin was eluted with 500 mM imidazole. Then, the peak fraction containing hemopexin was applied to a Sephacryl S-300 column (5 × 100 cm) in phosphate-buffered saline (PBS). Flow rates of 1 ml/min were obtained. Hemopexin in eluate fractions was determined by ELISA and the eluate fractions containing hemopexin were pooled and stored at -80°C. Purified plasma-derived hemopexin was characterized with SDS-PAGE and Western blotting (> 95% purity).

### *Thermal shock and microvesicle isolation*

Packed RBCs were resuspended in distilled H<sub>2</sub>O, Deferoxamine (DFO, Sigma), glutathione oxidized (GSSG, Sigma) or a platelet-poor plasma pool from healthy individuals (NHP, > 10 healthy donors) to a final hematocrit of 50%. The RBC suspension was subjected to 3 sequential freeze/thaw cycles to induce thermal shock and subsequent hemolysis. To obtain hemolytic microvesicles (HMVs), the RBC lysate was centrifuged at 20,000 g for 15 min at 4°C. Then, the HMV-containing fraction was washed twice with the corresponding assay buffer and the resulting pellet was resuspended to the original volume for further experiments.

### *Complement-mediated hemolysis and RBC sonication*

Complement-mediated hemolysis was induced as described previously<sup>1</sup>. In short, 1 × 10<sup>6</sup> bromelain-treated packed RBCs from a healthy donor were resuspended in 50 µL veronal buffer supplemented with 0.05% gelatin (VBG), 10 mM CaCl<sub>2</sub> and 2 mM MgCl<sub>2</sub> (VBG<sup>++</sup>). AIHA patient serum (with positive C3b score in the direct antiglobulin test) diluted in VBG for a final concentration of 10% (v/v) was incubated with the treated RBCs for 5 min to induce antibody

opsonization of the RBCs. Then, 25% (v/v) recalcified EDTA plasma from an AB blood group donor was added as source of complement factors in order to induce MAC formation and hemolysis. Alternatively, RBCs resuspended in assay buffer at 50% hematocrit were sonicated in a Branson model 220 cleaning sonicator (Shelton, CT) for 15 min at 37°C. The resulting RBC lysate after complement-mediated hemolysis and sonication was centrifuged for 15 min at 20,000 g to isolate the pellet containing HMVs for further experiments.

#### *Characterization of HMVs using flow cytometry and PS staining*

The purity of the HMV fraction was determined by fluorescent staining with the following antibodies: CD235a-phycoerythrin (PE) (Clone AME-1, CLB) CD14-Qdot® 800 (Clone TüK4, Life Technologies) and CD61-PECy7 (Clone SZ21, Beckman Coulter). To determine PS expression Lactadherin-FITC (milk fat globule EGF factor 8; Haematologics Technologies) staining was used. In short, HMVs isolated as described above and dissolved in phosphate buffered saline (PBS) were incubated with 50 µL FITC-lactadherin (final concentration 250-320 nM) and the antibodies (all diluted 1:50) or PBS (unstained control) for 20 min at room temperature. Then, HMVs were washed twice with PBS and resuspended in a final volume of 50 µL in PBS for analysis on a LSR/Fortessa (BD Bioscience). RBCs from the same healthy donor were used as negative control for PS expression within each experiment.

#### *Tissue factor pathway inhibitor (TFPI) depletion from plasma*

TFPI was depleted from NHP using the previously characterized monoclonal antibodies TFPI-6 and TFPI-15<sup>2</sup> directed against the Kunitz- 1 and 2 domain of TFPI, respectively. In short, NHP was incubated overnight at 4°C on a rotating platform with ~600 µg of each antibody coupled to CNBr-activated Sepharose® 4B (GE Healthcare). After centrifugation at 2500 rpm for 15 min, the supernatant containing TFPI-depleted plasma was collected and TFPI content was determined using ELISA. Briefly, Nunc Maxisorp® 96-well microtiter plates (Thermo Fischer) were coated overnight at room temperature with 2 µg/ml TFPI-6 antibody diluted in PBS. After washing the plates five times with PBS containing 0.02% Tween 20 (PBS-T), samples were diluted in high-performance ELISA (HPE) buffer (Sanquin Reagents), added to the plates in two-fold serial dilutions and incubated for 1 hour at room temperature on a shaker platform. The plates were then washed five times with PBS-T and incubated with 0.5 µg/ml biotinylated TFPI-15 antibody diluted in PBS-T supplemented with 1% normal mouse serum for 1 hour at 37°C. After washing with PBS-T, the plates were incubated with streptavidin poly-HRP (1:10,000 dilution in HPE buffer) for 25 min at room temperature on a shaker platform.



The ELISA was developed using 100 mg/mL 3,5,3'5'-tetramethylbenzidine in 0.1 M sodium acetate containing 0.003% (v/v) H<sub>2</sub>O<sub>2</sub>, pH 5.5 and the reaction was stopped with 100 mL 2 M H<sub>2</sub>SO<sub>4</sub>. Absorbance was measured at 450 and 540 nm with a Synergy 2 Multi-Mode plate reader (BioTek Instruments).

#### *Thrombin generation assay (TGA)*

Thrombin generation was determined using the calibrated automated thrombogram method<sup>3</sup> (Thrombinoscope, BV, The Netherlands). In short, 60 µL of NHP, Kininogen depleted plasma (Affinity Biologicals), Prekallikrein deficient plasma (CRYOcheck™, PrecisionBioLogic), FVII deficient plasma (Siemens diagnostics), Protein C deficient plasma (Hyphen BioMed) or TFPI-depleted NHP was supplemented with the indicated concentration HMVs (v/v %) and used to perform the TGA. To trigger coagulation activation, 20 µL PPP-low reagent (Thrombinoscope BV) containing 1 pM tissue factor (TF) and 4 µM synthetic phospholipids was added. After incubation of plasma with the starting reagent (37°C for 10 min), 20 µL of the fluorogenic thrombin-specific substrate Z-Gly-Gly-Arg-AMC (2.5 mM; Bachem) dissolved in N-2-hydroxyethylpiperazine-N9-2-ethanesulfonic acid buffer with bovine serum albumin and 100 mM CaCl<sub>2</sub> was used to start the clotting reaction by plasma recalcification. All samples were run in duplicate and fluorescence was monitored for 60 min using the Fluoroskan Ascent fluorometer (Thermo Labsystems).

#### *Western blot analysis*

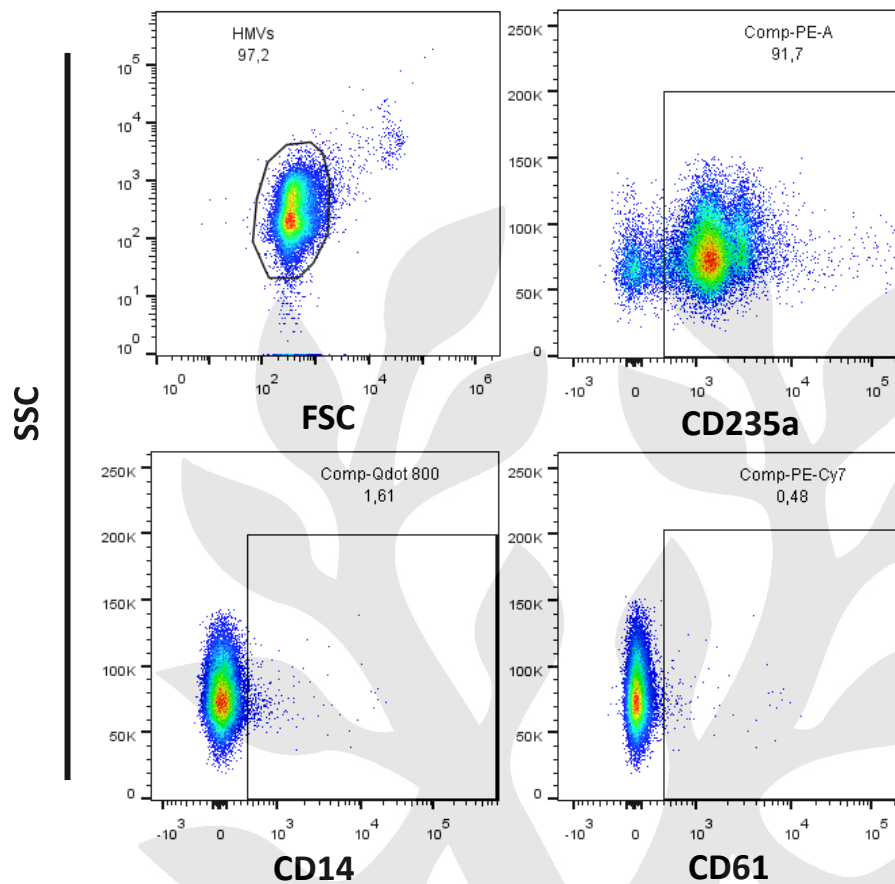
Expression of FXI, FXII and TF on the HMVs was assessed by Western blotting. The HMVs were generated as described above and diluted 10 and 100 times in PBS. 0.5 µg/mL human- FXII (Haematologic Technologies Inc) or FXI (Thermo Fisher Scientific) and 10 µl of the PPP-low reagent were used as positive controls. All samples were then incubated with NuPAGE Sample buffer solution (Invitrogen) at 70°C for 10 minutes and separated in a Novex NuPAGE 4-12% Bis-Tris gel under non-reducing conditions. As a loading control one gel was used for staining with InstantBlue™ (Expedeon) according to the manufacturer's instructions. For Western blotting, proteins were transferred to nitrocellulose membranes using the iblot™-System (Life Science Technologies) and blocked with 1% (v/v) Western Blocking Reagent (WBR, Roche) in PBS for 1 h. Membranes were then probed with 1 µg/mL of either polyclonal rabbit anti FXII antibody<sup>5</sup> or monoclonal mouse anti FXI-5 antibody<sup>4</sup> and 2 µg/mL rabbit polyclonal anti TF antibody (104513, Abcam). As secondary antibodies polyclonal swine anti rabbit IgG-HRP antibody or rabbit anti mouse IgG-HRP (1:500, both from Dako) were used.

After antibody incubation steps, proteins were detected using the Pierce™ ECL Plus Western Blotting Substrate (Thermo Fischer) and membranes were imaged using the Chemidoc MP imaging system (Bio-Rad).



## Supplementary figures

A



B

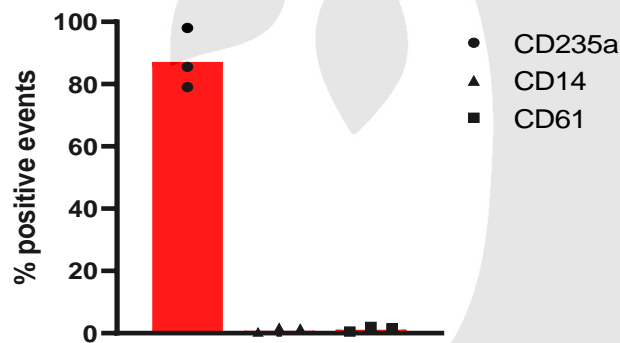


**Fig S1. Minimal contamination of isolated HMVs with platelets or monocytes.** Representative flow cytometry dot plots ( $n = 3$ ) showing the purity of enriched HMV fractions obtained by multiple freeze/thaw cycles (A). Forward and side scatter plot of isolated HMVs identifying the population of interest (top left panel) and dot plots showing RBC- (top right panel), monocyte- (bottom left) or platelet-derived (bottom right) vesicles in the HMV fraction after isolation using specific antibodies directed against CD235a, CD14 and CD61, respectively. (B) Percentage positive CD235a, CD14 and CD61 events from 3 RBC donors in the isolated HMV fraction.

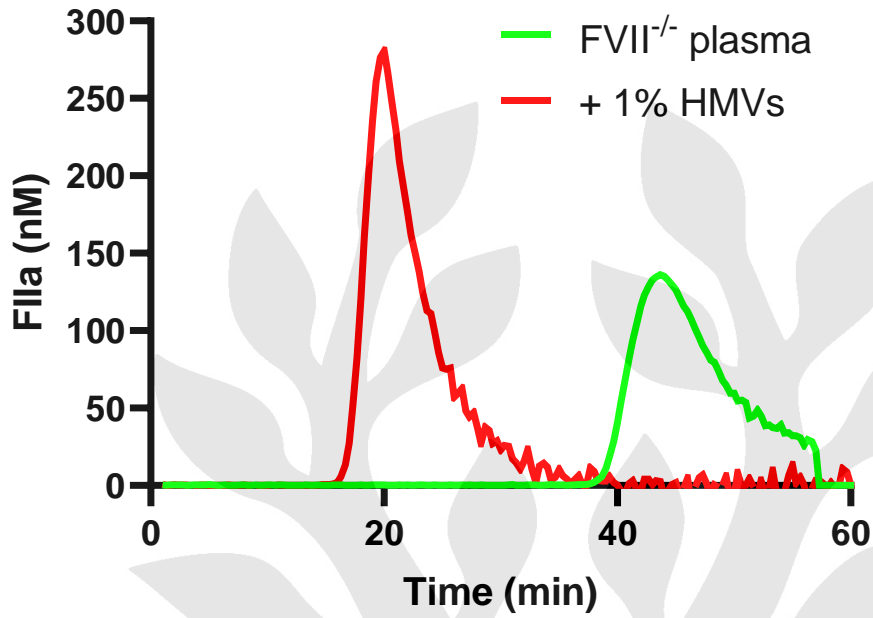


**Fig S2. HMVs increase thrombin generation independent of FVII.** Thrombin generation in FVII deficient plasma supplemented with 1% HMVs. Coagulation was initiated using 1 pM TF. Thrombogram is representative of 3 independent experiments.

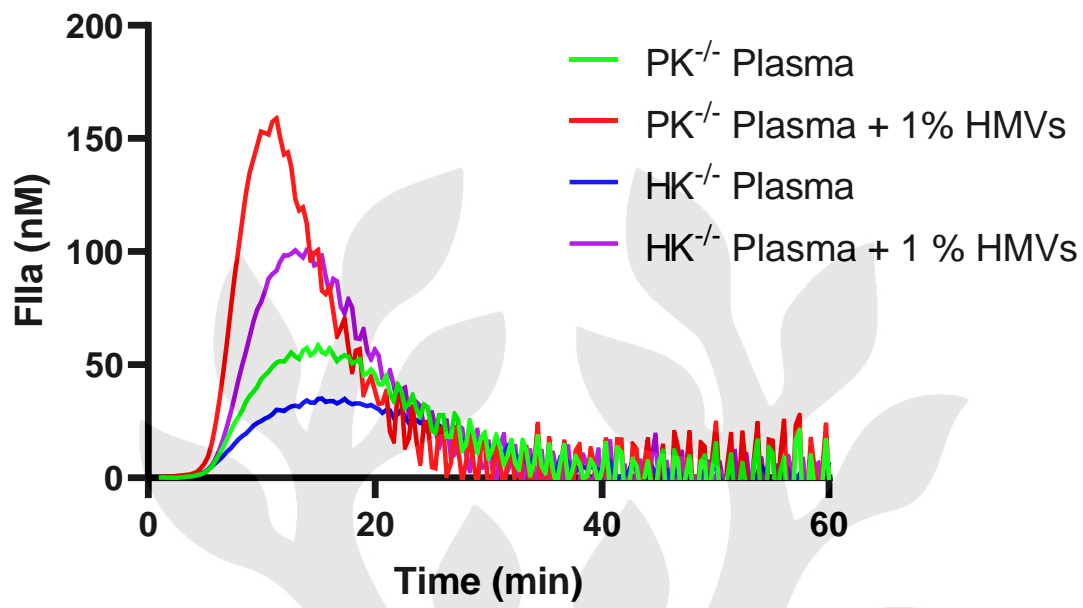
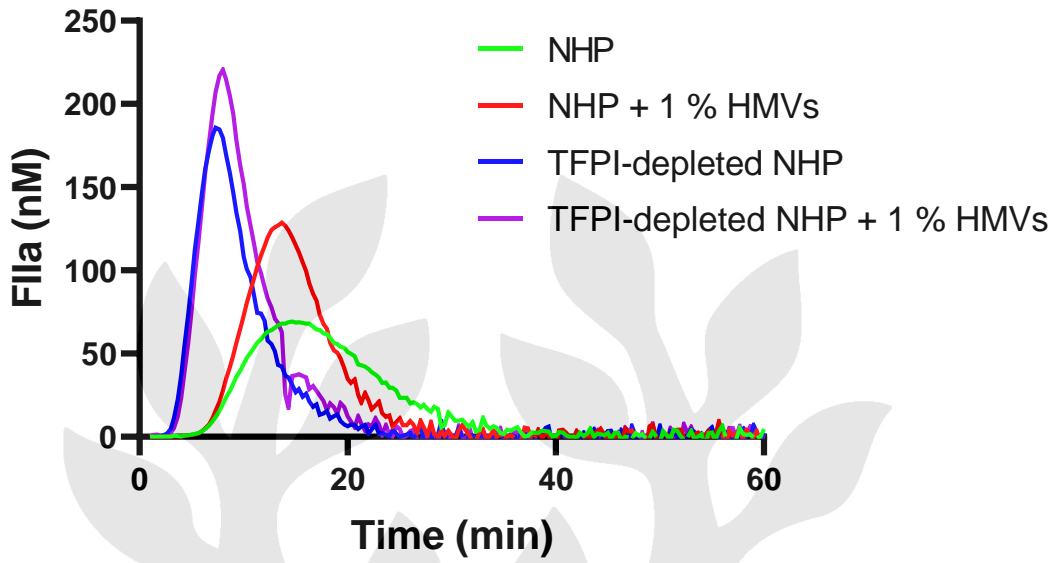


**Fig S3. HMVs increase thrombin generation independent of PK and HK.** Thrombin generation in PK and HK deficient plasma supplemented with 1 % HMVs. TGA was initiated using 1 pM TF. Results are representative of 2 independent experiments. PK: Prekallikrein., HK: High molecular weight kininogen.

A



B

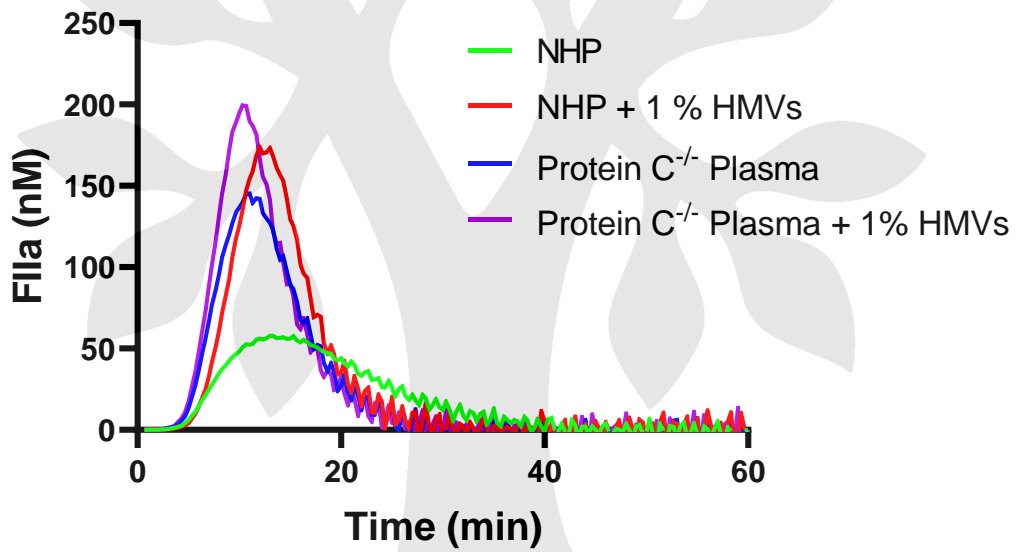
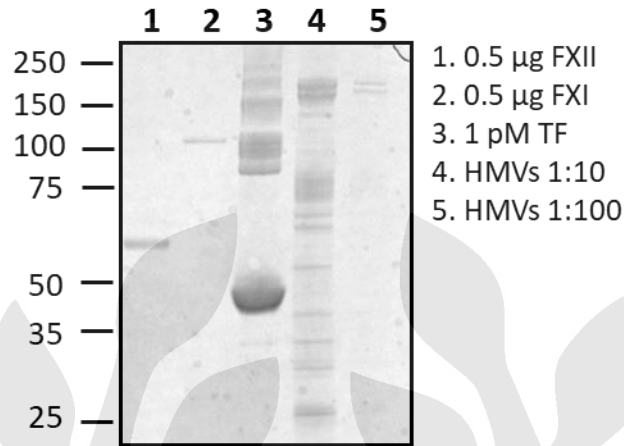


**Fig S4. HMVs increase thrombin generation in TFPI-depleted and Protein C deficient plasma.** Thrombin generation in NHP and (A) TFPI-depleted NHP or (B) Protein C deficient plasma either supplemented with 1% HMVs or untreated. TGA was initiated using 1 pM TF. Thrombograms are representative of 2 independent experiments. TFPI: Tissue factor pathway inhibitor.

**A**



**B**

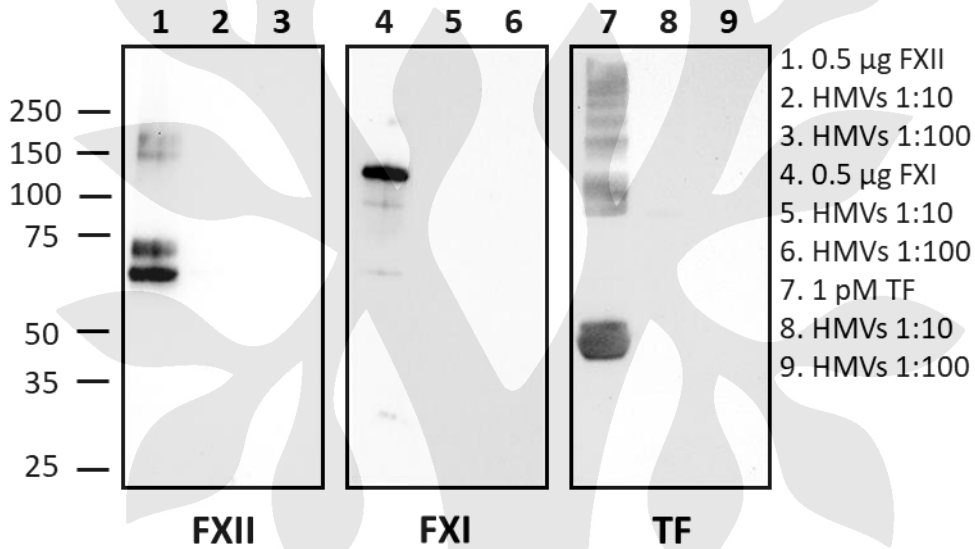
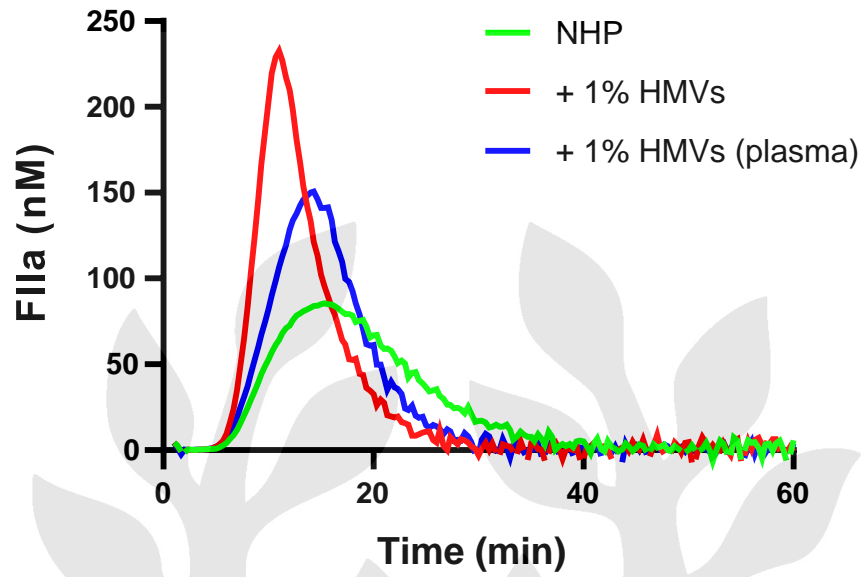


**Fig S5. HMVs do not express FXI, FXII and TF.** Expression of FXII, FXI and TF on HMVs diluted in PBS. (A). Non-reducing SDS-PAGE showing loaded HMVs and control proteins detected using Coomassie staining (B). Western Blots were probed with a polyclonal anti-FXII (left panel) monoclonal anti-FXI (central panel), or polyclonal anti-TF (right panel). Molecular weight standard is indicated.

A



B

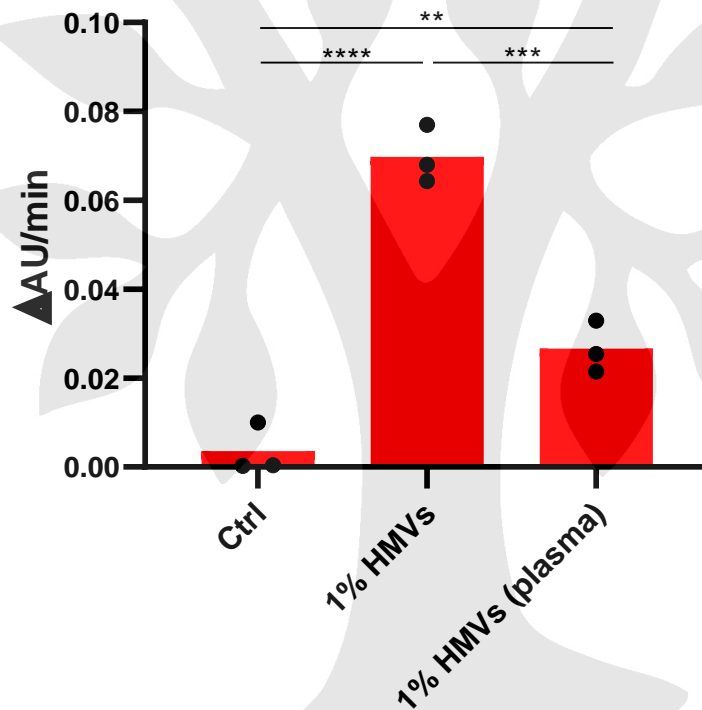


**Fig S6. RBC lysis in the presence of plasma reduces the effect of HMVs in the thrombin generation assay and FXa generation.** (A) Thrombin generation in NHP supplemented with 1% HMVs prepared in either distilled H<sub>2</sub>O or in the presence of plasma. Coagulation was initiated using 1 pM TF. Thrombogram is representative of 3 independent experiments. (B) FIXa and FVIIIa-dependent FXa generation in a purified system with 1% HMVs obtained in the presence of either buffer or plasma. FXa generation is depicted as delta arbitrary units per minute and data from 3 independent experiments are shown as mean with range. Statistical differences were calculated using the one-way ANOVA followed by Tukey post hoc test. A value of  $p < 0.05$  was considered statistically significant.



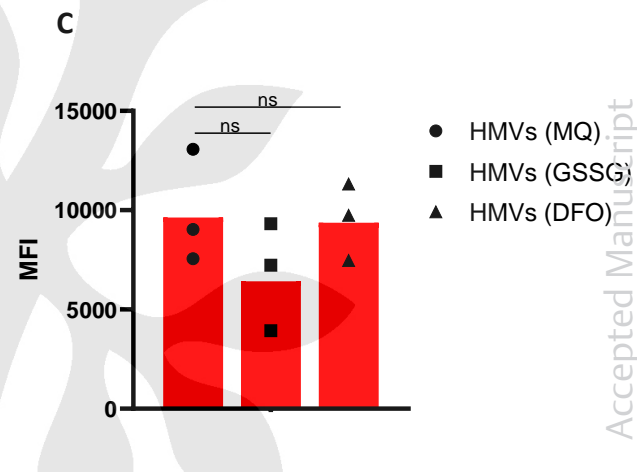
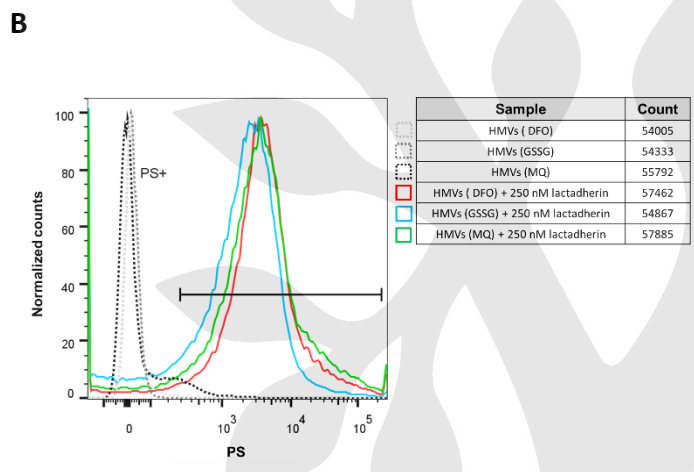
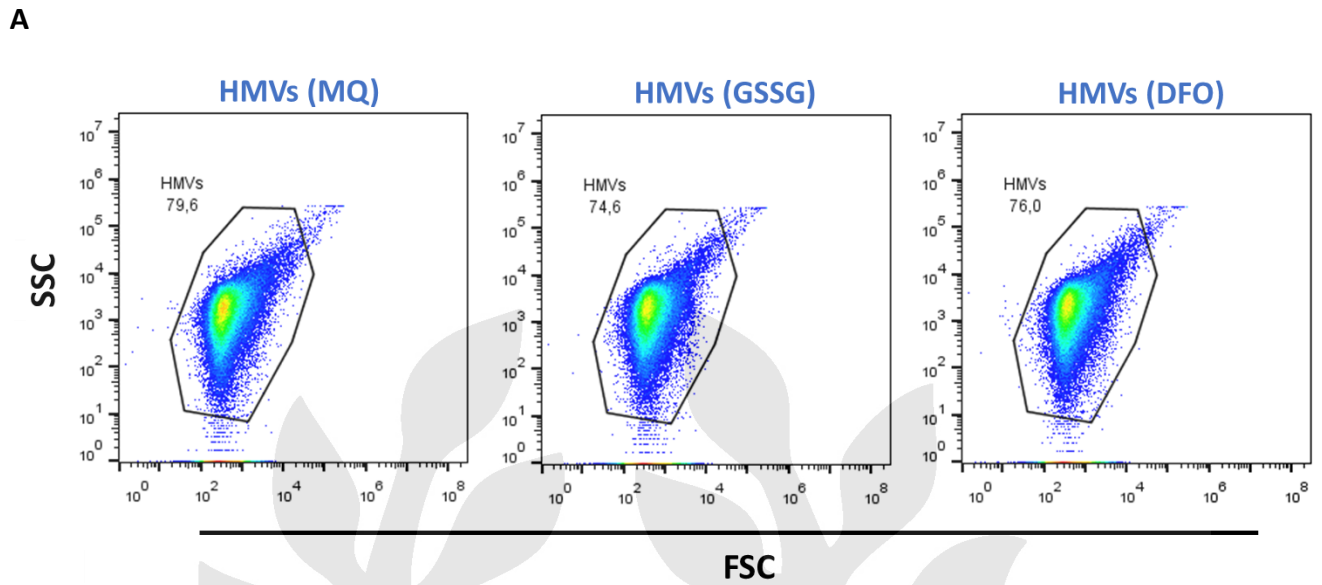


**Fig S7. Characterization of HMVs formed in the presence of different compounds.** RBCs were resuspended in either distilled H<sub>2</sub>O (MQ), glutathione (GSSG) or deferoxamine (DFO) and subjected to multiple freeze/thaw cycles before the formed HMVs were stained for PS exposure with 250 nM FITC-lactadherin and analyzed using flow cytometry. **(A)** Representative forward versus side scatter dot plots showing the percentage of formed HMVs from RBCs resuspended in the different compounds and **(B)** representative histogram (n=3) showing PS expression on these HMVs. **(C)** Mean fluorescence intensity values showing PS expression on the different HMVs from 3 different RBC donors.

## References

1. Baas I, Delvasto-Nuñez L, Ligthart P, et al. Complement C3 inhibition by compstatin Cp40 prevents intra- and extravascular hemolysis of red blood cells. *Haematologica*. 2020;105(2):e57-e60. Published 2020 Jan 31. doi:10.3324/haematol.2019.216028
2. Stephan F, Dienava-Verdoold I, Bulder I, Wouters D, Mast AE, Te Velthuis H, Aarden LA, Zeerleder S. Tissue factor pathway inhibitor is an inhibitor of factor VII-activating protease. *J Thromb Haemost*. 2012 Jun;10(6):1165-71. doi: 10.1111/j.1538-7836.2012.04712.x. PMID: 22449009; PMCID: PMC3574557.
3. Hemker HC, Giesen P, Al Dieri R, et al. Calibrated automated thrombin generation measurement in clotting plasma. *Pathophysiol Haemost Thromb*. 2003;33(1):4-15. doi:10.1159/000071636
4. Willemin WA, Minnema M, Meijers JC, Roem D, Eerenberg AJ, Nuijens JH, ten Cate H, Hack CE. Inactivation of factor XIa in human plasma assessed by measuring factor XIa-protease inhibitor complexes: major role for C1-inhibitor. *Blood*. 1995 Mar 15;85(6):1517-26. PMID: 7534133.
5. Nuijens JH, Huijbregts CC, Eerenberg-Belmer AJ, Abbink JJ, Strack van Schijndel RJ, Felt-Bersma RJ, Thijs LG, Hack CE. Quantification of plasma factor XIIa-C1(-)-inhibitor and kallikrein-C1(-)-inhibitor complexes in sepsis. *Blood*. 1988 Dec;72(6):1841-8. PMID: 3264190.

# Iron-driven alterations on red blood cell-derived microvesicles amplify coagulation during hemolysis via the intrinsic tenase complex

Laura Delvasto-Núñez<sup>1,2</sup>, Dorina Roem<sup>1</sup>, Kamran Bakhtiari<sup>3</sup>, Gerard van Mierlo<sup>1</sup>, Joost C. M. Meijers<sup>3,4</sup>, Ilse Jongerius<sup>1,5\*</sup> and Sacha S. Zeerleder<sup>1,6,7\*</sup>

<sup>1</sup>Department of Immunopathology, Sanquin Research and Landsteiner Laboratory, Amsterdam UMC, University of Amsterdam, Amsterdam, The Netherlands

<sup>2</sup>Department of Hematology, Amsterdam UMC, University of Amsterdam, Amsterdam, The Netherlands

<sup>3</sup>Department of Molecular and Cellular Hemostasis, Sanquin Research and Landsteiner Laboratory, Amsterdam UMC, University of Amsterdam, Amsterdam, The Netherlands

<sup>4</sup>Department of Experimental Vascular Medicine, Amsterdam UMC, University of Amsterdam, Amsterdam Cardiovascular Sciences, Amsterdam, The Netherlands

<sup>5</sup>Department of Pediatric Immunology, Amsterdam UMC, University of Amsterdam, Rheumatology and Infectious Diseases, Emma Children's Hospital, Amsterdam, The Netherlands

<sup>6</sup>Department of Hematology and Central Hematology Laboratory, Inselspital, Bern University Hospital, University of Bern, Switzerland

<sup>7</sup>Department for BioMedical Research, University of Bern, Switzerland

***\*These authors contributed equally.***

**Correspondence to:** Ilse Jongerius – Department of Immunopathology, Sanquin Research, Plesmanlaan 125, 1066 CX Amsterdam, The Netherlands – [i.jongerius@sanquin.nl](mailto:i.jongerius@sanquin.nl)

Sacha Zeerleder – Department of Hematology and Central Hematology Laboratory, Inselspital, Bern University Hospital, Freiburgstrasse 3, CH-3010 Bern, Switzerland – [sacha.zeerleder@insel.ch](mailto:sacha.zeerleder@insel.ch) –

**Classification:** Coagulation and Fibrinolysis

## Abstract

Hemolytic disorders characterized by complement-mediated intravascular hemolysis, such as autoimmune hemolytic anemia and paroxysmal nocturnal hemoglobinuria, are often complicated by life-threatening thromboembolic complications. Severe hemolytic episodes result in the release of red blood cell (RBC)-derived pro-inflammatory and oxidatively reactive mediators (e.g. extracellular hemoglobin, heme and iron) into plasma. Here, we studied the role of these hemolytic mediators in coagulation activation by measuring FXa and thrombin generation in the presence of RBC lysates. Our results show that hemolytic microvesicles (HMVs) formed during hemolysis stimulate thrombin generation through a mechanism involving FVIII and FIX, the so-called intrinsic tenase complex. Iron scavenging during hemolysis using deferoxamine decreased the ability of the HMVs to enhance thrombin generation. Furthermore, the addition of ferric chloride ( $\text{FeCl}_3$ ) to plasma propagated thrombin generation in a FVIII and FIX-dependent manner suggesting that iron positively affects blood coagulation. Phosphatidylserine (PS) blockade using lactadherin and iron chelation using deferoxamine reduced intrinsic tenase activity in a purified system containing HMVs as source of phospholipids confirming that both PS and iron ions contribute to the procoagulant effect of the HMVs. Finally, the effects of  $\text{FeCl}_3$  and HMVs decreased in the presence of ascorbate and glutathione indicating that oxidative stress plays a role in hypercoagulability. Overall, our results provide evidence for the contribution of iron ions derived from hemolytic RBCs to thrombin generation. These findings add to our understanding of the pathogenesis of thrombosis in hemolytic diseases.

**Keywords:** coagulation, red blood cells, iron, hemolysis, intrinsic tenase complex

## Introduction

Thromboembolic complications represent the most common complication of hemolytic disorders characterized by intravascular hemolysis such as paroxysmal nocturnal hemoglobinuria (PNH) and autoimmune hemolytic anemia (AIHA)<sup>1</sup>. Intravascular hemolysis is triggered by complement activation and the formation of the membrane attack complex on red blood cells (RBCs)<sup>2</sup>. Consequently, RBCs release pro-inflammatory danger associated molecular patterns (DAMPs) including extracellular hemoglobin, heme and iron<sup>3</sup>. These DAMPs accumulate in the vasculature during severe intravascular hemolytic episodes causing cell injury<sup>4</sup>. While an association between intravascular hemolysis and thrombosis has been proposed in AIHA<sup>5</sup>, the role of RBC-derived DAMPs in blood coagulation has not yet been fully elucidated. A reduced thrombotic risk in PNH patients treated with eculizumab<sup>6</sup>, an anti-C5 inhibitor that prevents membrane attack complex formation, and the crosstalk between the complement and coagulation pathways<sup>7</sup> suggest a role for complement in thrombosis. However, complement targeting in hemolytic anemias also reduces hemolysis<sup>8</sup>, hence it remains unclear whether the RBC-derived DAMPs also contribute to hypercoagulability.

Due to the pro-inflammatory nature of RBC-derived DAMPs, the human body is armed with a multi-component system to counteract hemolysis. First, plasma haptoglobin prevents oxidation of extracellular hemoglobin and the release of heme containing ferric iron ( $\text{Fe}^{3+}$ )<sup>9</sup>. Second, the plasma glycoprotein hemopexin scavenges free heme with subsequent internalization of the hemopexin-heme complex avoiding inflammation and iron loss<sup>10</sup>. Finally, heme oxygenases act as rate-limiting enzymes in the intracellular degradation of heme leading to the generation of carbon monoxide, biliverdin and ferrous iron ( $\text{Fe}^{2+}$ )<sup>12</sup>.  $\text{Fe}^{2+}$  is captured by ferritin for oxidation into  $\text{Fe}^{3+}$  and intracellular storage<sup>11</sup> and plasma transferrin binds circulating  $\text{Fe}^{3+}$  thereby enabling its transport and preventing the formation of reactive oxygen species<sup>12</sup>. During severe hemolytic episodes, the neutralizing capacity of the scavengers is overwhelmed as shown by decreased concentrations of circulating haptoglobin and hemopexin<sup>13</sup> and high transferrin saturation<sup>14</sup>. Consequently, oxidative stress represents one of the most significant effects of chronic hemolysis<sup>15,16</sup>.

Next to oxidative damage, hemolysis also results in the formation of hemolytic microvesicles (HMs). HMs are small RBC-derived vesicles highly abundant in individuals suffering from hemolytic anemias<sup>17</sup> with presumably enhanced procoagulant properties when compared to vesicles derived from other cellular sources<sup>18</sup>. HMs originate from the plasma membrane and are composed of membrane proteins and phospholipids including phosphatidylserine (PS)<sup>19</sup>. Exposure of PS on HMs can function as a signal for phagocytosis<sup>19</sup> but also as template for coagulation reactions which has been demonstrated in PNH<sup>20,21</sup>. To investigate the effect of hemolysis and the generated RBC-derived DAMPs on coagulation activation, we used the thrombin generation assay (TGA). TGAs have been shown to accurately reflect the overall hemostatic phenotype and being of great value in the evaluation of (venous) thrombotic tendencies in plasma<sup>22</sup>. Coagulation is initiated by the extrinsic tenase complex that consist of tissue factor (TF) and activated FVII (FVIIa) and cleaves FX into FXa<sup>23</sup>. Plasma clotting can also be triggered by the (auto)activation of FXII upon contact with negatively charged surfaces<sup>24</sup>. Activation of this pathway (known as intrinsic coagulation) leads to FXIIa-mediated generation of FXIa which in turn activates FIX generating FIXa. FIXa then binds to FVIIIa forming the intrinsic tenase complex that cleaves FX resulting in FXa generation<sup>24</sup>. Thus, activation of either the extrinsic or intrinsic tenase complex will lead to FXa generation, the formation of the prothrombinase complex (i.e. FXa and FVa) and subsequent thrombin generation.

It has been shown that RBC-derived microvesicles (MVs) activate FXII<sup>25,26</sup> and prekallikrein<sup>25</sup> directly and potentiate coagulation by a FXI-mediated mechanism<sup>27</sup>. We here show that HMs promote thrombin generation by an intrinsic tenase complex-dependent manner. Next, we show that, through a mechanism involving membrane phospholipids on HMs and oxidative stress, iron ions derived from hemolytic RBCs propagate coagulation via the intrinsic tenase complex. Overall, our data suggest a possible role for iron ions originating from hemolytic RBCs on blood coagulation and provide insights into the mechanisms behind the high thrombotic incidence in hemolytic diseases.

## Materials and methods

Supplemental material contains an additional description of methods and is available online.

### *HMV isolation*

Written informed consent was obtained for all used blood samples according to the declaration of Helsinki. Citrated whole blood was collected from healthy volunteers and RBCs were isolated as described previously<sup>28</sup>. Packed RBCs were resuspended in distilled H<sub>2</sub>O or assay buffer to a final hematocrit of 50%. The RBC suspension was subjected to 3 sequential freeze/thaw cycles to induce thermal shock and subsequent hemolysis. In a set of experiments, packed RBCs were resuspended to a final hematocrit of 50% in either plasma, 50  $\mu$ M deferoxamine (DFO; Sigma-Aldrich), 0.5 mg/mL haptoglobin (Sigma-Aldrich), 1 mg/mL hemopexin (see Supplemental Methods), 5-25 mM glutathione oxidized (GSSG; Sigma-Aldrich) or 1-5 mM ascorbate (Merck) before subjecting the cells to hemolysis. The resulting RBC lysate was centrifuged for 5 min at 1800 rpm and the supernatant was collected. To obtain HMVs, the RBC lysate was centrifuged at 20,000 g for 15 min at 4°C. Then, the HMV-containing fraction was washed three times with the corresponding assay buffer to remove excess inhibitors and prevent additional effects in the TGA. The resulting pellet was resuspended to the original volume for further experiments.

### *TGA*

Thrombin generation was determined using the calibrated automated thrombogram method<sup>29</sup> (Thrombinoscope, BV, The Netherlands) as described previously<sup>30</sup>. In short, 60  $\mu$ L of a platelet-poor plasma pool from healthy donors (> 10 individuals), further referred to as normal human plasma (NHP), was supplemented with the indicated concentration HMVs (v/v). Alternatively, FXI-, FXII- (both from Haematologic Technologies), FVII-, FVIII-, FIX- (all from Siemens Healthcare Diagnostics), FX- or FV- (both from George King Bio-Medical) deficient plasmas were used for supplementation with HMVs. In a set of experiments, MVs were depleted from NHP by centrifugation at 20,000 g for 15 min at 4°C. Plasma-derived MVs were treated with 10  $\mu$ M FeCl<sub>3</sub> (Sigma-Aldrich) for 10 min, washed (20,000 g for 15 min at 4°C) and used to supplement MV-free plasma in their original volume. Samples were diluted with 20  $\mu$ L assay buffer (50 mM Tris/150 mM NaCl pH 7.4).

In some experiments  $\text{FeCl}_3$  was used to supplement NHP, FVIII or FIX deficient plasma. In some experiments 20  $\mu\text{g}/\text{mL}$  neutralizing antibodies against FVIII (clone VK34<sup>31</sup>) or FIX (clone 5F5<sup>32</sup>) were pre-incubated with NHP. To trigger coagulation, 20  $\mu\text{L}$  of one of the following reagents were added: PPP-low (1  $\mu\text{M}$  TF), PPP reagent (5  $\mu\text{M}$  TF), MP (4  $\mu\text{M}$  synthetic phospholipids), or 8  $\mu\text{M}$  FIXa<sup>32</sup> dissolved in MP reagent. After incubation of plasma with the starting reagent (37°C for 10 min), 20  $\mu\text{L}$  of the fluorogenic thrombin-specific substrate Z-Gly-Gly-Arg-AMC (2.5 mM; Bachem) dissolved in N-2-hydroxyethylpiperazine-N9-2-ethanesulfonic acid buffer with bovine serum albumin and 100 mM  $\text{CaCl}_2$  was used to start the clotting reaction by plasma recalcification. All samples were run in duplicate and fluorescence was monitored for 60 min using the Fluoroskan Ascent fluorometer (Thermo Labsystems). The following parameters were derived from the thrombograms according to Hemker<sup>30</sup>: 1) the peak thrombin concentration, 2) the velocity index (efficiency of thrombin generation), 3) the endogenous thrombin potential (ETP or area under the thrombin curve) and 4) the lag time (time between initiation and the moment at which 10 nM thrombin is formed).

#### *Chromogenic assay for intrinsic tenase activity*

A modified version of the two-stage FVIIIa COATEST<sup>®</sup> SP (Chromogenix) was used to determine FVIIIa cofactor activity. In short, a reagent containing FIXa + FX (Chromogenix) and recombinant FVIII (0.1 U/mL; Sanquin) were incubated with phospholipids (Chromogenix) or HMVs for 5 min at 37°C. Then, thrombin (1 nM; Sigma-Aldrich) and  $\text{CaCl}_2$  (1.5 mM) were added to the mixture to activate FVIII. After addition of the chromogenic substrate S-2765<sup>™</sup> (0.45 mM; Chromogenix) FXa generation was determined by measuring the rate of substrate hydrolysis (change in absorbance at 405 nm) in a Multiskan<sup>™</sup> FC Microplate Photometer (Thermo Labsystems). All experiments were carried out in duplicate.

#### *Statistical analysis*

Differences in coagulation parameters between the control NHP condition and treated or supplemented NHP were analyzed using the student *t* test. Statistical differences between multiple groups were calculated using the one-way ANOVA followed by Tukey post hoc test. A value of  $p < 0.05$  was considered statistically significant. GraphPad Prism 7.0 software was used for graphical



representation and statistical analysis. Flow cytometry data were analyzed using FlowJo software v.10 (FlowJo).

## Results

### HMVs increase thrombin generation independent of the method used to induce hemolysis

To investigate the role of RBC-derived DAMPs on coagulation, RBCs were subjected to hemolysis by thermal shock and the RBC lysate was used to supplement NHP for determination of thrombin generation. The RBC lysate enhanced thrombin generation in a dose-dependent manner (Fig. **1A**). To determine which constituents promote thrombin generation, two fractions were isolated from the RBC lysate using ultracentrifugation: the hemolytic supernatant and a fraction consisting of HMVs. Platelet and monocyte contamination in the isolated HMV fraction was excluded using flow cytometry (**Supplemental Fig. 1**). Procoagulant changes in NHP were solely observed with the HMV fraction (Fig. **1B**). These changes were reflected in significantly higher peak height ( $191 \pm 30$  nM vs.  $78 \pm 14$  nM), velocity index ( $40.7$  nM/min  $\pm 14.6$  vs.  $9.5 \pm 2.1$  nM/min) and ETP ( $1478 \pm 177$  nM.min vs.  $1206 \pm 190$  nM.min). Addition of untreated RBCs to NHP did not affect thrombin generation whereas, similar to the effects observed with thermal shock-induced HMVs, HMVs obtained after sonication of RBCs or by complement-induced hemolysis enhanced thrombin generation (Fig. **1D**). This indicates that HMVs potentiate thrombin generation independent of the method applied to induce hemolysis.

### HMVs propagate thrombin generation via the intrinsic tenase complex

To determine which coagulation pathway is involved in the HMV-enhanced thrombin generation varying concentrations TF were used to trigger coagulation in the TGA. When high concentrations TF ( $> 5$  pM) are used to trigger the TGA mainly the extrinsic pathway plays a role whereas in the absence of TF or when using a relatively low concentration (1pM), the intrinsic pathway is the main driver of thrombin generation. Addition of HMVs to NHP did not result in increased thrombin levels when 5 pM TF was used to initiate TGAs (Fig. **2A**), whilst HMVs

significantly amplified thrombin formation in the absence of TF as well as in the presence of 1pM TF (Fig. 2A). This points towards an effect of HMVs involving the intrinsic coagulation pathway.

In case certain coagulation factors are involved in the observed HMV-enhanced thrombin generation, removing them from the system will result in loss of the procoagulant effect of the HMVs. We therefore systematically assessed the role of intrinsic coagulation factors by supplementing FXII, FXI, FIX or FVIII deficient plasma with HMVs and determined thrombin generation. Comparable to the effect on NHP, increased thrombin generation was observed in FXII or FXI deficient plasma supplemented with HMVs (Fig. 2B), indicating that FXII and FXI do not play a major role in the observed effects. Interestingly, HMVs were unable to potentiate thrombin generation in these FVIII or FIX deficient plasma suggesting that the intrinsic tenase complex is involved in the procoagulant effect of the HMVs (Fig. 2C). These results were confirmed by incorporating neutralizing antibodies directed against FIX or FVIII in NHP. In the presence of these antibodies, the HMVs failed to augment thrombin levels (Fig. 2D-E). To rule out that the so called “Josso loop”<sup>33</sup> (activation of FIX by FVIIa) was key in the effect of the HMVs, TGA was also determined in FVII deficient plasma supplemented with HMVs. An increment of thrombin generation was observed in the absence of FVII (**Supplemental Fig. 2**) indicating that the presence of FVII is not required for the HMV-driven effect. While kallikrein has been proposed to trigger FXI-independent FIX activation<sup>25,34</sup>, we found that HMVs increased thrombin generation in prekallikrein and high molecular weight kininogen deficient plasma (**Supplemental Fig. 3**), hence involvement of these proteins in our system is not likely. Similarly, the HMVs had a procoagulant effect in plasma lacking tissue factor pathway inhibitor (TFPI) or Protein C (**Supplemental Fig. 4**) which suggests that HMV enhance thrombin generation independently of these coagulation inhibitors. Collectively, these data suggest that HMVs act via the intrinsic tenase complex.

Next, to investigate whether HMVs activate FIX directly, we supplemented FIX deficient plasma with HMVs and added FIXa to start the TGA. Elevated thrombin levels were found after the addition of HMVs to this FIX deficient plasma (Fig. 2F) indicating that the HMVs act downstream FIXa. Irrespective of the addition of the HMVs, thrombin generation was absent in FX deficient

plasma (data not shown). Pro-coagulant extracellular MVs derived from different cellular sources including platelets and RBCs circulate in plasma<sup>18,19</sup>. Irrespective of the presence of the HMVs, no thrombin generation could be detected in TGAs without TF as starting reagent when MV-depleted NHP was used (data not shown). Furthermore, we were not able to detect FXII, FXI and TF in our HMV fraction using Western blot analysis (**Supplemental Fig. 5**). These results suggest that no coagulation activating compound is present in the HMV fraction. Thus, in our system it seems that the HMVs do not active coagulation directly but rather contribute to the thrombin burst in NHP via the intrinsic tenase complex.

### **HMVs potentiate thrombin generation through a mechanism involving PS and iron ions**

Hemolysis results in exposure of PS<sup>20,21</sup> and the release of RBC-derived DAMPs<sup>5</sup>. To determine whether PS contributes to HMV-potentiated thrombin generation, we first detected PS expression on HMVs using lactadherin. As expected, untreated RBCs were largely PS negative<sup>19</sup> while HMVs formed after subjecting the same RBCs to thermal shock express PS (Fig. **3A**). To establish whether PS exposed on the HMVs facilitates intrinsic tenase activity, we determined FXa generation by the intrinsic tenase complex in a purified system consisting of either phospholipids or HMVs as unique source of PS. FXa was generated in the presence of phospholipids or HMVs in this system (Fig. **3B**). FXa generation was completely blocked by adding 100 nM lactadherin to phospholipids, whereas residual FXa generation was still present when the same concentration lactadherin was used to block PS exposure on HMVs (Fig. **3B**). Thus, the HMV-driven FXa generation is partially PS dependent but other mechanisms seem to be involved.

As discussed, next to PS exposure, hemolysis also results in the release of RBC-derived DAMPs which can bind to and alter the RBC plasma membrane<sup>35-37</sup>. To assess whether hemoglobin and hemopexin contribute to HMV-enhanced thrombin generation, we first subjected RBCs to hemolysis in the presence of haptoglobin and hemopexin, the physiological inhibitors of hemoglobin and heme respectively<sup>9</sup>. Addition of haptoglobin (Fig. **3C**) or hemopexin (Fig. **3D**) during hemolysis had no effect on the procoagulant effects of the HMVs. Next, to assess the role of iron ions in the HMV-driven effects, HMVs were formed in the presence of DFO, an iron chelator used for the

treatment of iron overload<sup>38</sup>. DFO reduced the procoagulant effect of the HMVs in the TGA (Fig. 3E) suggesting the participation of iron in HMV-driven thrombin generation. Similar results were obtained when RBCs were subjected to hemolysis in the presence of plasma (Supplemental Fig. 6A) which contains the physiological iron scavengers apotransferrin and ferritin. Addition of DFO to HMVs after their preparation had no effect on the procoagulant effects of the HMVs in the TGA (data not shown) suggesting that only real time iron chelation reduces HMV-enhanced thrombin generation. Overall, these data indicate that iron ions derived from hemolytic RBCs play a role in the procoagulant effects of HMVs.

### **Iron promotes coagulation via a mechanism involving the intrinsic tenase complex**

To verify the involvement of iron in coagulation, we supplemented NHP with FeCl<sub>3</sub> and determined thrombin generation in the TGA. Addition of FeCl<sub>3</sub> led to a dose-dependent increase in thrombin generation (Fig. 4A) and pre-incubation of FeCl<sub>3</sub> with DFO reversed thrombin levels to nearly those in NHP alone (Fig. 4B). As we showed that HMVs activate thrombin via the intrinsic tenase complex, we next investigated whether iron also acts at the level of this complex by blocking FVIII or FIX activity in NHP using neutralizing antibodies. Similar to the HMVs, FeCl<sub>3</sub> failed to enhance thrombin generation in NHP lacking functional FVIII and FIX (Fig. 4C-D). To confirm these results, we evaluated the ability of HMVs formed in the presence of DFO, in order to chelate iron ions, to facilitate intrinsic tenase activity and subsequently FXa generation in a purified system. Compared to HMVs obtained in buffer, less FXa was generated with DFO- (Fig. 4E) and plasma-formed HMVs (Supplemental Fig. 6B). No differences were found in PS expression and total counts between HMVs formed in the presence or absence of DFO (Supplemental Fig. 7). This points towards a role for iron, derived from hemolytic RBCs, in the intrinsic tenase activity. Incubation of HMVs generated in the presence of DFO with lactadherin further reduced FXa generation (Fig. 4E) suggesting that both PS exposure on HMVs and RBC-derived iron contribute to intrinsic tenase activity. In conclusion, we demonstrated a role for iron ions in blood clotting via the intrinsic tenase complex.

### **The procoagulant effect of iron is dependent on phospholipids and oxidative stress**

Next, we sought to assess the mechanism for iron-enhanced thrombin generation. Considering that interactions of  $\text{Fe}^{3+}$  with membrane phospholipids have been shown previously<sup>39</sup> and that PS was involved in the observed effects as well (Fig. 3B), we hypothesized that the presence of MVs containing PS was essential for iron-enhanced thrombin generation. Extracellular MVs derived from different cellular sources including platelets and RBCs circulate in human plasma<sup>18,19</sup>. Therefore, to test whether MVs are involved in the effects of  $\text{FeCl}_3$ , we centrifuged NHP and collected the MV-free supernatant for TGA experiments. Addition of  $\text{FeCl}_3$  to MV-free NHP did not result in increased thrombin levels but replenishment of this NHP with  $\text{FeCl}_3$ -treated plasma-derived MVs restored the procoagulant phenotype (Fig. 5A). These data point towards an effect of  $\text{FeCl}_3$  on plasma-derived MVs resulting in potentiated thrombin generation. To evaluate whether  $\text{FeCl}_3$  acts on membrane phospholipids directly, we supplemented MV-free NHP with  $\text{FeCl}_3$ -treated phospholipids and performed TGAs. Irrespective of the addition of  $\text{FeCl}_3$ , no thrombin generation was observed in MV-free NHP in the absence of synthetic phospholipids (Fig. 5B). Phospholipids treated with  $\text{FeCl}_3$  enhanced thrombin generation compared to untreated phospholipids suggesting that membrane phospholipids are involved in the effect of  $\text{Fe}^{3+}$  on coagulation (Fig. 5B).

As it has been shown that iron ions oxidize  $\text{PS}^{39}$ , we sought to investigate whether oxidative stress is involved in the effect of the HMVs. HMVs obtained in the presence of ascorbate (Fig. 5C) and GSSG (Fig. 5D) were less able to increase thrombin generation in NHP compared to untreated HMVs even though PS expression was similar independent of the presence of antioxidants (Supplemental Fig. 7). Additionally, the activity of HMVs in the FXa generation assay was reduced when HMVs were formed in the presence of the same antioxidants (Fig. 5E). Overall, these results imply that phospholipids are essential for the effects of  $\text{FeCl}_3$  in the TGA most likely via oxidative processes.

## Discussion

Here, we show that HMVs support thrombin generation via the intrinsic tenase complex and demonstrate that next to PS, a known player in coagulation<sup>40-42</sup>, also iron ions originating from

hemolytic cells play a role in blood clotting. In the absence of plasma scavengers, hemolysis results in the release of RBC-derived DAMPs including extracellular hemoglobin, heme and iron, and the formation of HMVs<sup>3,17</sup>. We here show that addition of HMVs, but not hemolytic supernatant, to NHP increased thrombin levels. This is in agreement with previous studies showing that RBC-derived MVs have procoagulant activity<sup>25-27</sup>. Previous reports have attributed these procoagulant effects to direct activation of FXII<sup>25,26</sup> and prekallikrein<sup>25</sup>, and to FXI-dependent thrombin generation<sup>27</sup>. Although we used comparable concentrations of RBC-derived MVs to the study by Rubin *et al.*, we show that the effect of HMVs is mediated by the intrinsic tenase complex independently of FXII and FXI. This could be partially explained by the differences in the origin of the RBC-derived MVs used in the different studies. While we subjected RBCs to thermal shock or complement-mediated hemolysis, others have obtained RBC-derived MVs by storage lesion-induced damage<sup>25,27</sup> or using Ca<sup>2+</sup> ionophores<sup>26</sup>. To mimic the hemolytic disintegration of RBCs as observed during complement-mediated hemolytic episodes, we opted for a system independent of Ca<sup>2+</sup> ionophores and long-term stored RBCs. **In our experimental conditions, we were unable to detect FXII and FXI on the HMVs using WB (Supplemental Fig. 5), which is in line with a previous study on the RBC proteome<sup>43</sup>. However, we cannot exclude that trace amounts of bound FXII or FXI are present on the RBCs and might contribute to the observed potentiation of thrombin generation.**

Another discrepancy between our data and previous studies is the direct activation of coagulation factors by RBC-derived MVs. A recent study showed RBC-derived MV-driven thrombin generation in the absence of a coagulation trigger by direct activation of prekallikrein and subsequent FIXa generation independent of FXI<sup>25</sup>. HMVs in our study however, are active in the absence of prekallikrein (**Supplemental Fig. 3**) and act downstream of FIXa (Fig. **2F**). No evidence was found for cleavage of FIX or prekallikrein directly by a proteolytic enzyme, as neither trypsin nor proteinase K treatment of the HMVs affected thrombin levels in the TGA (data not shown).

In agreement with previous studies, we have shown that PS is a major player in the procoagulant activity of HMVs<sup>20,21</sup>. PS on MVs induces FXII activation<sup>40</sup>, the formation of prothrombinase complexes<sup>41</sup> and the assembly and activity of the intrinsic tenase complex<sup>42</sup>. In our

experimental conditions, we only found an effect of PS-expressing HMVs on FVIIIa/FIXa activity. The explanation for this remains unknown.

Since altered RBC membranes have been described after exposure to RBC-derived DAMPs<sup>35-37</sup>, we assessed their role in the effects of HMVs in TGA. Neither haptoglobin nor hemopexin affected HMV-enhanced thrombin generation indicating that hemoglobin and heme were not directly involved in the observed effects. A partial reduction in thrombin generation in the TGA was achieved by the addition of NHP (**supplemental Fig. 6**) and by iron chelation using DFO (**Fig. 3E**) during hemolysis. This demonstrates that iron ions rather than heme and hemoglobin potentiate thrombin generation. We indeed showed that addition of FeCl<sub>3</sub> resulted in a dose-dependent increase in thrombin generation, which was blocked by addition of DFO (**Fig. 4B**). The selected concentrations FeCl<sub>3</sub> in our experiments (1-10 μM) are in the range of “chelatable” and thus reactive plasma iron levels in hemolytic disease<sup>44</sup>. Therefore, we postulate that the effects found in this study might be of relevance in hemolytic patients.

In a purified system, we determined that HMVs facilitate intrinsic tenase complex assembly allowing FXa generation (**Fig. 3B**). However, the HMV-mediated FXa generation by the intrinsic tenase complex was slightly lower compared to that of phospholipids (**Fig. 3B**). This could be explained by the relatively low concentration of HMVs used in the assay (to mimic physiological hemolytic levels) as compared to synthetic phospholipids. Interestingly, HMV-dependent FXa generation was partially reduced by iron chelation during hemolysis with DFO, by PS blockade using lactadherin and by dual inhibition. This indicates that both iron and PS participate in the procoagulant effects of the HMVs. Iron chelation and lactadherin did not have an additive effect on FXa activity when used together (**Fig. 4E**). We hypothesize that incorporation of lactadherin might not have an additional effect since lactadherin presumably is still able to bind to phosphatidylserine independent of the oxidation state. Hence, compared to lactadherin alone, a combination of DFO and lactadherin possibly does not result in significantly reduced FXa activity. In line with our findings, others have shown iron-mediated generation of thick fibrin fibers with increased resistance for fibrinolysis<sup>45</sup> and adhesion of RBCs to the endothelium after exposure to FeCl<sub>3</sub> in the FeCl<sub>3</sub>-induced arterial thrombosis murine model<sup>46</sup>. To our knowledge, we are the first to demonstrate a role for iron on intrinsic tenase

complex activity. We postulate that iron ions cause PS peroxidation on the HMVs, which in turn potentiates the procoagulant properties of PS as it was recently shown that enzymatically oxidized phospholipids promote coagulation<sup>47</sup>. During hemolytic episodes, iron represents a source of oxidative stress as it has been shown that Fe<sup>3+</sup> can oxidize membrane phospholipids<sup>39</sup>. This is supported by the fact that thrombin generation in plasma and FXa generation decreased in our study by the antioxidants ascorbate and GSSG (Fig. 5D-E). Others have shown that redox reactive iron directly induces PS peroxidation on cell membranes causing ferroptosis<sup>48</sup> illustrating the potential deleterious effects of labile iron *in vivo*. Although we have not investigated the source of redox reactive iron in our system, there are two plausible options: 1) heme-derived iron<sup>49</sup> and 2) the small labile iron pool stored in RBCs<sup>50</sup>. In the absence of physiological regulators of RBC-derived DAMPs, hemolysis leads to the release of ferrous heme which is instantly oxidized with subsequent accumulation of ferric heme<sup>49</sup>. These heme-iron species oxidize organic compounds in the presence of hydrogen peroxide (Fenton chemistry)<sup>49</sup>. However, since hemopexin does not affect HMV-enhanced thrombin generation it is not likely that heme-iron will contribute to the observed effects in this study. It is possible that compartmentalized labile iron in RBCs is released during hemolysis<sup>50</sup> causing the observed effects but this needs to be confirmed in future studies.

HMVs were shown to potentiate thrombin generation even in the absence of FVII (Supplemental Fig. 2). Furthermore, as we could not detect TF on our HMV fraction (Supplemental Fig. 5) and since it is widely accepted that RBCs do not express TF<sup>28</sup> we concluded that involvement of the extrinsic pathway is less likely. This is in contrast to a previous study showing heme-induced coagulation activation due to a TF-dependent mechanism<sup>51</sup>. We report here that the intrinsic tenase complex and thus not TF is determinant for HMV-potentiated thrombin generation in our cell-free system.

Intravascular hemolysis correlates with detrimental clinical outcomes and thrombosis-associated mortality in AIHA<sup>5</sup>. We found that HMVs isolated after complement-mediated hemolysis using AIHA sera also increase thrombin generation. Our results might be of importance in the pathogenesis of thrombosis in AIHA but evidence for this should further be studied in a physiologically more relevant system. The evidence found in this study suggest, however, that



oxidation of phospholipids by iron results in a surface that potentiates FVIII/FIX activity towards FX and therefore potentiates thrombin generation. Oxidative stress in PNH has been shown previously<sup>21</sup> but data on the oxidative status of AIHA patients are scarce, partially due to the clinical heterogeneity of the disease<sup>5</sup>. This underscores the need for a suitable system to study the pathophysiology of AIHA. Our study has some limitations. Hemolysis in the presence of DFO and antioxidants is not sufficient to completely abolish the procoagulant effect of the HMVs, which might indicate that other unidentified effectors contribute to hemolysis-associated hypercoagulability as well.

## Conclusion

The results of this study suggest the participation of iron ions, derived from disintegrated RBCs during hemolysis, in coagulation through FVIII/FIX interactions involving oxidative reactions. Our findings provide insights into the effect of hemolysis on the pathogenesis of thrombosis in patients suffering from chronic hemolytic anemia in diseases such as AIHA and PNH. The physiological relevance of these findings should be further explored *in vivo*.

<p><b>What is known about this topic?</b></p>	<ul style="list-style-type: none"> <li>• Complement-mediated hemolytic diseases characterized by intravascular hemolysis are associated with hypercoagulability and an increased incidence of thrombosis</li> <li>• Complement targeting in complement-driven hemolytic anemias reduces hemolysis and thromboembolic manifestations</li> <li>• The contribution of hemolytic mediators such as extracellular heme and iron to blood coagulation and the subsequent development of thrombosis remains elusive</li> </ul>
<p><b>What does this paper add?</b></p>	<ul style="list-style-type: none"> <li>• Hemolytic microvesicles (HMVs) formed during lysis of erythrocytes act via the intrinsic tenase complex potentiating thrombin generation</li> <li>• Hemolysis-derived iron ions contribute to HMV-enhanced thrombin generation</li> <li>• Iron-induced lipid peroxidation of membrane phospholipids is a potential mechanism behind the procoagulant effects of iron.</li> </ul>

## **Acknowledgments**

This study was supported by research funding from Trombosetiching Nederland to SZ (grant number 201604) and by a Product and Process Development grant obtained (in competition) from Sanquin Blood Supply Foundation (PPOC19-24/L2467) to IJ.

## **Authorship Contributions**

LDN, JM, IJ and SZ conceptualized the study and contributed to the design and execution of the research. IJ and SZ obtained funding for the study. LDN, DR, KB performed the experiments and analyzed the data; LDN, DR, KB, GM, JM, IJ and SZ interpreted the data and designed the experiments. LDN, JM, IJ and SZ wrote the initial draft of the manuscript and all authors critically commented on the manuscript.

## **Conflict of Interest Disclosures**

The authors declare no competing financial interests

## References

1. Ataga KI. Hypercoagulability and thrombotic complications in hemolytic anemias. *Haematologica*. 2009;94(11):1481-1484. doi:10.3324/haematol.2009.013672
2. Brodsky RA. Complement in hemolytic anemia. *Hematology Am Soc Hematol Educ Program*. 2015;2015:385-391. doi:10.1182/asheducation-2015.1.385
3. Rother RP, Bell L, Hillmen P, Gladwin MT. The clinical sequelae of intravascular hemolysis and extracellular plasma hemoglobin: a novel mechanism of human disease. *JAMA*. 2005;293(13):1653-1662. doi:10.1001/jama.293.13.1653
4. Mendonça R, Silveira AA, Conran N. Red cell DAMPs and inflammation. *Inflamm Res*. 2016;65(9):665-678. doi:10.1007/s00011-016-0955-9
5. Barcellini W, Fattizzo B, Zaninoni A, et al. Clinical heterogeneity and predictors of outcome in primary autoimmune hemolytic anemia: a GIMEMA study of 308 patients. *Blood*. 2014;124(19):2930-2936. doi:10.1182/blood-2014-06-583021
6. Hillmen P, Muus P, Dührsen U, et al. Effect of the complement inhibitor eculizumab on thromboembolism in patients with paroxysmal nocturnal hemoglobinuria. *Blood*. 2007;110(12):4123-4128. doi:10.1182/blood-2007-06-095646
7. Oikonomopoulou K, Ricklin D, Ward PA, Lambris JD. Interactions between coagulation and complement--their role in inflammation. *Semin Immunopathol*. 2012;34(1):151-165. doi:10.1007/s00281-011-0280-x
8. Wouters D, Zeerleder S. Complement inhibitors to treat IgM-mediated autoimmune hemolysis. *Haematologica*. 2015;100(11):1388-1395. doi:10.3324/haematol.2015.128538
9. Schaer DJ, Buehler PW, Alayash AI, Belcher JD, Vercellotti GM. Hemolysis and free hemoglobin revisited: exploring hemoglobin and heme scavengers as a novel class of therapeutic proteins. *Blood*. 2013;121(8):1276-1284. doi:10.1182/blood-2012-11-451229
10. Gozzelino R, Jeney V, Soares MP. Mechanisms of cell protection by heme oxygenase-1. *Annu Rev Pharmacol Toxicol*. 2010;50:323-354. doi:10.1146/annurev.pharmtox.010909.105600
11. Knovich, M. A., Storey, J. A., Coffman, L. G., Torti, S. V., & Torti, F. M. Ferritin for the clinician. *Blood reviews*. 2019;23(3), 95–104. <https://doi.org/10.1016/j.blre.2008.08.001>
12. Parkkinen J, von Bonsdorff L, Ebeling F, Sahlstedt L. Function and therapeutic development of apotransferrin. *Vox Sang*. 2002;83 Suppl 1:321-326. doi:10.1111/j.1423-0410.2002.tb05327.x
13. Muller-Eberhard U, Javid J, Liem HH, Hanstein A, Hanna M. Plasma concentrations of hemopexin, haptoglobin and heme in patients with various hemolytic diseases. *Blood*. 1968;32(5):811-815
14. Santiago RP, Guarda CC, Figueiredo CVB, et al. Serum haptoglobin and hemopexin levels are depleted in pediatric sickle cell disease patients. *Blood Cells Mol Dis*. 2018;72:34-36. doi:10.1016/j.bcmd.2018.07.002
15. Fibach E, Rachmilewitz EA. Iron overload in hematological disorders. *Presse Med*. 2017;46(12 Pt 2):e296-e305. doi:10.1016/j.lpm.2017.10.007
16. Fibach E, Dana M. Oxidative stress in paroxysmal nocturnal hemoglobinuria and other conditions of complement-mediated hemolysis. *Free Radic Biol Med*. 2015;88(Pt A):63-69. doi:10.1016/j.freeradbiomed.2015.04.027

17. Alaarg A, Schiffelers RM, van Solinge WW, van Wijk R. Red blood cell vesiculation in hereditary hemolytic anemia. *Front Physiol.* 2013;4:365. 2013 Dec 13. doi:10.3389/fphys.2013.00365
18. Hugel B, Socié G, Vu T, Toti F, Gluckman E, Freyssinet JM, Scrobohaci ML. Elevated levels of circulating procoagulant microparticles in patients with paroxysmal nocturnal hemoglobinuria and aplastic anemia. *Blood.* 1999 May 15;93(10):3451-6. PMID: 10233897.
19. Connor J, Pak CC, Schroit AJ. Exposure of phosphatidylserine in the outer leaflet of human red blood cells. Relationship to cell density, cell age, and clearance by mononuclear cells. *J Biol Chem.* 1994;269(4):2399-2404
20. Kozuma Y, Sawahata Y, Takei Y, Chiba S, Ninomiya H. Procoagulant properties of microparticles released from red blood cells in paroxysmal nocturnal haemoglobinuria. *Br J Haematol.* 2011 Mar;152(5):631-9. doi: 10.1111/j.1365-2141.2010.08505.x. Epub 2011 Jan 17. PMID: 21241275.
21. Ninomiya H, Kawashima Y, Hasegawa Y, Nagasawa T. Complement-induced procoagulant alteration of red blood cell membranes with microvesicle formation in paroxysmal nocturnal haemoglobinuria (PNH): implication for thrombogenesis in PNH. *Br J Haematol.* 1999;106(1):224-231. doi:10.1046/j.1365-2141.1999.01483.x
22. Brummel-Ziedins KE, Vossen CY, Butenas S, Mann KG, Rosendaal FR. Thrombin generation profiles in deep venous thrombosis. *J Thromb Haemost.* 2005;3(11):2497-2505. doi:10.1111/j.1538-7836.2005.01584.x
23. Smith SA, Travers RJ, Morrissey JH. How it all starts: Initiation of the clotting cascade. *Crit Rev Biochem Mol Biol.* 2015;50(4):326-336. doi:10.3109/10409238.2015.1050550
24. Renné T, Gailani D. Role of Factor XII in hemostasis and thrombosis: clinical implications. *Expert Rev Cardiovasc Ther.* 2007;5(4):733-741. doi:10.1586/14779072.5.4.733
25. Noubouossie DF, Henderson MW, Mooberry M, et al. Red blood cell microvesicles activate the contact system, leading to factor IX activation via 2 independent pathways. *Blood.* 2020;135(10):755-765. doi:10.1182/blood.2019001643
26. Van Der Meijden PE, Van Schilfgaarde M, Van Oerle R, Renné T, ten Cate H, Spronk HM. Platelet- and erythrocyte-derived microparticles trigger thrombin generation via factor XIIa. *J Thromb Haemost.* 2012;10(7):1355-1362. doi:10.1111/j.1538-7836.2012.04758.x
27. Rubin O, Delobel J, Prudent M, et al. Red blood cell-derived microparticles isolated from blood units initiate and propagate thrombin generation. *Transfusion.* 2013;53(8):1744-1754. doi:10.1111/trf.12008
28. Baas I, Delvasto-Nuñez L, Ligthart P, et al. Complement C3 inhibition by compstatin Cp40 prevents intra- and extravascular hemolysis of red blood cells. *Haematologica.* 2020;105(2):e57-e60. Published 2020 Jan 31. doi:10.3324/haematol.2019.216028
29. Hemker HC, Giesen P, Al Dieri R, et al. Calibrated automated thrombin generation measurement in clotting plasma. *Pathophysiol Haemost Thromb.* 2003;33(1):4-15. doi:10.1159/000071636
30. Dinkelaar J, Molenaar PJ, Ninivaggi M, de Laat B, Brinkman HJ, Leyte A. In vitro assessment, using thrombin generation, of the applicability of prothrombin complex concentrate as an antidote for Rivaroxaban. *J Thromb Haemost.* 2013 Jun;11(6):1111-8. doi: 10.1111/jth.12236. PMID: 23578206.
31. Herczenik E, van Haren SD, Wroblewska A, et al. Uptake of blood coagulation factor VIII by dendritic cells is mediated via its C1 domain. *J Allergy Clin Immunol.* 2012;129(2):501-509.e5095. doi:10.1016/j.jaci.2011.08.029

32. Bakhtiari K, Meijers JCM. In vitro evaluation of factor IX as novel treatment for factor XI deficiency. *Blood*. 2019;134(6):573-575. doi:10.1182/blood.2019000681
33. Joso F, Prou-Wartelle O. Interaction of tissue factor and factor VII at the earliest phase of coagulation. *Thromb Diath Haemorrh Suppl*. 1965;17:35-44
34. Visser M, van Oerle R, Ten Cate H, Laux V, Mackman N, Heitmeier S, Spronk HMH. Plasma Kallikrein Contributes to Coagulation in the Absence of Factor XI by Activating Factor IX. *Arterioscler Thromb Vasc Biol*. 2020 Jan;40(1):103-111. doi: 10.1161/ATVBAHA.119.313503. Epub 2019 Nov 26. PMID: 31766871.
35. Jeney V, Balla J, Yachie A, et al. Pro-oxidant and cytotoxic effects of circulating heme. *Blood*. 2002;100(3):879-887. doi:10.1182/blood.v100.3.879
36. Omodeo Salè F, Vanzulli E, Caielli S, Taramelli D. Regulation of human erythrocyte glyceraldehyde-3-phosphate dehydrogenase by ferriprotoporphyrin IX. *FEBS Lett*. 2005;579(22):5095-5099. doi:10.1016/j.febslet.2005.07.081
37. Chu H, McKenna MM, Krump NA, et al. Reversible binding of hemoglobin to band 3 constitutes the molecular switch that mediates O<sub>2</sub> regulation of erythrocyte properties. *Blood*. 2016;128(23):2708-2716. doi:10.1182/blood-2016-01-692079
38. Olivieri NF, Brittenham GM. Iron-chelating therapy and the treatment of thalassemia [published correction appears in *Blood* 1997 Apr 1;89(7):2621]. *Blood*. 1997;89(3):739-761
39. Dacaranhe CD, Terao J. A unique antioxidant activity of phosphatidylserine on iron-induced lipid peroxidation of phospholipid bilayers. *Lipids*. 2001;36(10):1105-1110. doi:10.1007/s11745-001-0820-7
40. Yang A, Chen F, He C, et al. The Procoagulant Activity of Apoptotic Cells Is Mediated by Interaction with Factor XII. *Front Immunol*. 2017;8:1188. Published 2017 Sep 25. doi:10.3389/fimmu.2017.01188
41. Majumder R, Quinn-Allen MA, Kane WH, Lentz BR. A phosphatidylserine binding site in factor Va C1 domain regulates both assembly and activity of the prothrombinase complex. *Blood*. 2008;112(7):2795-2802. doi:10.1182/blood-2008-02-138941
42. van Dieijen G, Tans G, Rosing J, Hemker HC. The role of phospholipid and factor VIIIa in the activation of bovine factor X. *J Biol Chem*. 1981;256(7):3433-3442
43. Pasini EM, Kirkegaard M, Mortensen P, Lutz HU, Thomas AW, Mann M. In-depth analysis of the membrane and cytosolic proteome of red blood cells. *Blood*. 2006 Aug 1;108(3):791-801. doi: 10.1182/blood-2005-11-007799. PMID: 16861337.
44. Esposito BP, Breuer W, Sirankapracha P, Pootrakul P, Hershko C, Cabantchik ZI. Labile plasma iron in iron overload: redox activity and susceptibility to chelation. *Blood*. 2003;102(7):2670-2677. doi:10.1182/blood-2003-03-0807
45. Lipinski B, Pretorius E, Oberholzer HM, Van Der Spuy WJ. Iron enhances generation of fibrin fibers in human blood: implications for pathogenesis of stroke. *Microsc Res Tech*. 2012;75(9):1185-1190. doi:10.1002/jemt.22047
46. Barr JD, Chauhan AK, Schaeffer GV, Hansen JK, Motto DG. Red blood cells mediate the onset of thrombosis in the ferric chloride murine model. *Blood*. 2013;121(18):3733-3741. doi:10.1182/blood-2012-11-468983
47. Lauder SN, Allen-Redpath K, Slatter DA, et al. Networks of enzymatically oxidized membrane lipids support calcium-dependent coagulation factor binding to maintain hemostasis. *Sci Signal*. 2017;10(507):eaan2787. Published 2017 Nov 28. doi:10.1126/scisignal.aan2787

48. Dixon S & Stockwell B. The Hallmarks of Ferroptosis. *Annu Rev Cancer Biol.* 2019;3. 10.1146/annurev-cancerbio-030518-055844
49. Carlsen C, Møller J & Skibsted L. Heme-iron in lipid oxidation. *Coord Chem Rev.* 2005;249:485-498. 10.1016/j.ccr.2004.08.028
50. Prus E, Fibach E. The labile iron pool in human erythroid cells. *Br J Haematol.* 2008;142(2):301-307. doi:10.1111/j.1365-2141.2008.07192.x
51. Sparkenbaugh EM, Chantrathammachart P, Wang S, et al. Excess of heme induces tissue factor-dependent activation of coagulation in mice. *Haematologica.* 2015;100(3):308-314. doi:10.3324/haematol.2014.114728

**Fig 1. HMVs increase thrombin generation.** (A) Thrombograms showing thrombin generation in NHP supplemented with different concentrations RBC lysate (0.5-2%) obtained by thermal shock. (B) Thrombin generation in NHP supplemented with either 2% RBC lysate or 2% HS and HMV fractions obtained after ultracentrifugation of the RBC lysate. (C) Coagulation parameters in NHP supplemented with 1% HMVs obtained by thermal shock. (D) Peak thrombin levels in NHP supplemented with 1% HMVs obtained by either subjecting RBCs to thermal shock, sonication, complement-mediated hemolysis or with untreated RBCs. Coagulation was initiated using 1 pM TF in all experiments. Thrombograms are representative of at least 3 independent experiments and data are expressed as mean with range.

**Fig 2. HMVs affect thrombin generation via the intrinsic pathway involving FVIII and FIX.** (A) Peak thrombin levels in NHP supplemented with 1% HMVs after the addition of different concentrations TF (0-5 pM) to start the TGA. Data from 3 independent experiments are expressed as mean with range. (B) Representative thrombograms showing thrombin generation in FXII (green lines) or FXI deficient plasma (red lines) either supplemented with 1% HMVs (dotted lines) or untreated (solid lines). (C) Representative thrombograms showing thrombin generation in FVIII (green lines) or FIX (red lines) deficient plasma either supplemented with 1% HMVs (dotted lines) or untreated (solid lines). Thrombin generation in NHP untreated or incubated with 20 µg/mL neutralizing antibodies against (D) FVIII or (E) FIX in the presence or absence of 1% HMVs. (F) Thrombin generation in FIX deficient plasma supplemented with 1% HMVs or untreated after addition of 8 pM FIXa. Coagulation was initiated using 1 pM TF (B-E) and thrombograms are representative of at least 3 independent experiments.

**Fig 3. PS expression and iron derived from hemolytic RBCs exert procoagulant effects.** HMVs and RBCs were stained for PS exposure with 320 nM FITC-lactadherin and analyzed using flow cytometry. (A) Representative histogram showing PS expression on HMVs and RBCs. (B) FXa generation in the presence of 1% HMVs or phospholipids (PLs) either pre-incubated with 100 nM lactadherin or untreated. FXa generation is depicted as delta arbitrary units per minute and data from 3 independent experiments are shown as mean with range. Thrombin generation in NHP supplemented with 1% HMVs obtained after thermal shock-induced hemolysis of RBCs in the presence of (C) 0.5 mg/mL haptoglobin, (D) 1 mg/mL hemopexin, or (E) 50 µM DFO. Thrombograms are representative of at least 3 independent experiments.

**Fig 4. Iron ions potentiate coagulation via a mechanism involving the intrinsic tenase complex.** (A) Thrombograms showing thrombin generation in NHP supplemented with increasing concentrations FeCl<sub>3</sub> (1-100 μM). (B) Thrombin generation in NHP supplemented with 10 μM FeCl<sub>3</sub> in the presence of 50 μM DFO. Thrombin generation in NHP untreated or incubated with 20 ug/mL neutralizing antibodies against (C) FVIII or (D) FIX in the presence or absence of 10 μM FeCl<sub>3</sub>. Coagulation was initiated using 1 pM TF in TGAs and thrombograms are representative of at least 3 independent experiments. (E) FXa generation in the presence of 1% HMVs either obtained in the presence of 50 μM DFO, or incubated with 50 nM lactadherin or both. FXa generation is depicted as delta arbitrary units per minute and data from 3 independent experiments are shown as mean with range.

**Fig 5. Iron ions potentiate coagulation through interactions with membrane phospholipids and oxidative stress.** (A) Thrombograms of untreated or MV-free NHP supplemented with 10 μM FeCl<sub>3</sub> alone or after replenishment with plasma-derived MVs either treated with 10 μM FeCl<sub>3</sub> or untreated. (B) Thrombin generation in MV-free NHP supplemented with 10 μM FeCl<sub>3</sub>, 8 μM synthetic phospholipids (PLs) or both. Thrombin generation in NHP supplemented with 1% HMVs obtained in the presence of either (C) 1 mM ascorbate or (D) 5 mM GSSG. Coagulation was initiated using 1 pM TF (A, C, D) or without the addition of any coagulation trigger (B). Thrombograms are representative of at least three independent experiments. (E) FXa generation in the presence of 1% HMVs obtained by lysing RBCs in the presence of either buffer, 5mM ascorbate or 25mM GSSG. FXa generation is depicted as delta arbitrary units per minute and data from 3 independent experiments are shown as mean with range.